

UNIVERSITY OF OKLAHOMA

GRADUATE COLLEGE

COMPARATIVE SEM ANALYSIS OF QUARTZ MICROTERTURES ON
FLUVIAL SAND FROM END-MEMBER CLIMATE SYSTEMS

A THESIS

SUBMITTED TO THE GRADUATE FACULTY

in partial fulfillment of the requirements for the

Degree of

MASTER OF SCIENCE

By

CURTIS SMITH
Norman, Oklahoma
2016

COMPARATIVE SEM ANALYSIS OF QUARTZ MICROTERTURES ON
FLUVIAL SAND FROM END-MEMBER CLIMATE SYSTEMS

A THESIS APPROVED FOR THE
CONOCOPHILLIPS SCHOOL OF GEOLOGY AND GEOPHYSICS

BY

Dr. Gerilyn S. Soreghan, Chair

Dr. Michael S. Soreghan

Dr. Megan E. Elwood Madden

© Copyright by CURTIS SMITH 2016
All Rights Reserved.

Acknowledgements

First, I would like to thank Dr. Lynn Soreghan. None of this would have been possible without her endless vigor and passion. She was always there to push me, provide another great idea, or teach me something new, whether it be in the jungle of Puerto Rico or in her office for our weekly meeting. I thank her even more for her enormous patience in carefully reviewing every version of this thesis and dealing with all the unnecessary and (probably much too often) deleterious writing that came with it.

I thank my committee members Dr. Mike Soreghan and Dr. Megan Elwood-Madden for all of their great ideas, constructive comments, providing papers, and reviewing of this thesis. Furthermore, I would like to thank Dr. Tohru Ohta of Waseda University, Tokyo, and Dr. Brad Wallet and Dr. Steve Westrop of OU for their aid in statistics. As a complete novice in statistics, their help was invaluable in analysis of my samples. I thank Dr. Young Ji Joo for all of her help with preparing samples, looking over my figures, geochemical expertise, and constructive comments. Her help was invaluable for the completion of this project.

I thank Dr. Preston Larson of the Sam Noble Electron Laboratory for teaching me how to use the SEM and his patience in helping prepare my samples. Gary Stowe of the Integrated Core Characterization Center for further training on the SEM and his valuable advice on micro-imaging. And fellow OU students Alyssa Wickard and Gerry Heij for further SEM assistance.

I thank my mother for all of her phone calls and unending support through all the ups and down over the past two years.

I would like to thank fellow student Ann Ojeda for her enthusiasm and being a sounding board for all my thoughts and idea, both academic and not. Molly Sexton, Jeffrey Westrop, and Xiao Qi for being fantastic office mates and friends.

Lastly I would like to thank L. Davila and G. Martel for field assistance in Peru. C. Portocarrero Rodriguez for permitting, logistical support, and technical advice. R. J. Gomez López for organizing permit 157-2015-SERNANP-PNH/J to Huascarán National Park, Peru. A. Velez and F. Cartagena of the University of Puerto Rico Mayagüez for field assistance in Puerto Rico. L. Murray, L. Bellah, and B. Edely for organizing DPR065 Permit 208 for Anza-Borrego State Park. I. Kvalen and M. Knagenhjelm for organizing our permit for Jostedalsbreen National Park.

This work was funded by ACS PRF grant # 52114-ND8 and NSF grant # EAR-1225126 awarded to Dr. Gerilyn Soreghan. Additional support was provided by the James Roy Maxey Professorship.

Table of Contents

Acknowledgements.....	iv
List of Tables	viii
List of Figures.....	ix
Abstract.....	x
Introduction.....	1
Geological Background and Study Areas.....	4
Puerto Rico.....	4
Norway.....	5
Anza-Borrego, California	6
Peru	7
Methods.....	9
Initial Research Design	9
Field Sampling.....	10
Laboratory Processing	11
Principal Component Analysis	13
Results of Microtexture Analysis.....	16
Univariate Location Results.....	16
Principal Component Analysis	17
All Textures	17
Mechanical Textures.....	19
Summary.....	20
Ternary Analysis.....	21

Discussion.....	22
Comparisons with Previous Studies	22
Application of Quartz Microtextures as a Climate Proxy.....	24
Complexity of Natural Systems.....	27
Methodological Recommendations	28
Conclusions.....	30
References Cited.....	32
Appendix A: Tables	45
Appendix B: Figures.....	54
Appendix C: Microtexture Count Raw Data	67

List of Tables

Table 1. Bedrock lithologic details of the sample sites.....	45
Table 2. Climate, transect, and basin details of study sites.....	46
Table 3. Sample sizes and size fractions used in previous microtextural studies.....	47
Table 4. Microtexture descriptions, abbreviations, and inferred formation processes...	48
Table 5. Mean occurrence and standard deviation of microtextures for each location..	49
Table 6. Eigenvalues and variance for both PCA runs.....	51
Table 7. Loadings of the PCA results representing all textures.....	52
Table 8. Loadings of the PCA results representing mechanical textures.....	53

List of Figures

Figure 1. Geologic maps of the study locations.....	54
Figure 2. Photos from each study location.....	56
Figure 3. Selected microtextures documented in this study.....	57
Figure 4. More selected microtextures documented in this study.....	59
Figure 5. Line graph of percussion induced fractures.....	61
Figure 6. Plots from PCA analysis of all textures.....	63
Figure 7. Plots from PCA analysis of mechanical textures.....	64
Figure 8. Ternary Plot.....	65
Figure 9. Venn diagram	66

Abstract

Microtextural analyses of sedimentary quartz grains are increasingly used as a paleoenvironmental proxy, as particular microtextures have been proposed to reflect processes unique to particular environmental or climatic conditions. However, little consensus exists on which microtextures may be unique to a particular weathering process, and what types of quantitative approaches are needed to use this approach for paleoclimate reconstruction. This study documents microtextures on fluvial quartz grains collected in modern end-member climates (with respect to precipitation and temperature) to assess whether climate imparts unique microtextures (or suites of microtextures) potentially useful for interpreting paleoclimate. To isolate climate as the primary variable, other attributes such as bedrock lithology, transect length, and drainage basin size, were controlled to the degree possible in an empirical comparison. Presence of 17 microtextures on first-cycle quartz from fluvial systems in Puerto Rico (hot-humid), Norway (cold-humid-proglacial), California (hot-arid), and Peru (cold-semiarid-proglacial), was documented under double-blind conditions, and results analyzed using principal component analysis (PCA). Results from PCA, combined with univariate analysis results, were used to construct a ternary diagram to enable visual comparison of large datasets. Humid and arid climates are statistically distinct on the basis primarily of common precipitation features and secondarily, v-shaped percussion fractures, the former caused by enhanced chemical weathering and the latter by fluvial saltation. Grains from arid climates exhibit a larger incidence of upturned plates, interpreted to reflect the influence of high-stress aeolian saltation on grains that subsequently undergo fluvial entrainment. Grains from proglacial systems exhibit a

higher incidence of fracture faces, possibly attributable to the effects of both freeze-thaw weathering and glacial crushing. However, with the exceptions of the humid-arid distinction, differences in microtextural suites are subtle. These results suggest that quartz microtextural analysis holds some promise for aiding paleoclimatic interpretations for coarse-grained fluvial strata, but additional research is needed to assess whether additional methodological approaches to grain analyses and/or statistical techniques could further strengthen climatic differentiation.

Introduction

The advent and increasing use of electron microscopy in the 1960s inspired early attempts to determine depositional environments using microtextures on quartz grains (e.g., Biederman, 1962; Krinsley and Takahashi, 1962; Porter, 1962; Krinsley and Donahue, 1968). After significant work in this area, however, researchers realized that many different types of processes occurring during transport and deposition can produce similar types of textures — the concept of “equifinality” (Brown, 1973; Gomez and Small, 1983; Mahaney, 2002). Subsequently, efforts to assess depositional environment using SEM microtextural analysis fell out of favor.

More recently, two factors have driven a revival in these efforts. Firstly, further research has suggested that certain textures record relatively unique processes that do reflect particular environments or transportation processes. Whereas textures such as conchoidal fracturing, steps, and fracture faces can be induced in a number of ways, microstriae, for example, have been hypothesized as relatively unique to glacially influenced systems (Mahaney and Kalm, 2000; Mahaney, 2002). Secondly, the increasing use of quantitative data analyses can reveal trends otherwise hidden in the data, akin to conducting statistical analyses of taphonomic data in paleobiology (Kowalewski et al., 1995; Kowalewski and Labarbera, 2004), quantitative particle shape analysis (Blott and Pye, 2007), and Fourier and principal component analysis on sand grain shape (Thomas et al., 1995; Suzuki et al., 2015). For example, Deane (2010) employed statistical analyses of microtextural data on sample sizes of 100-150 grains from Quaternary deposits of unknown origin to argue for the influence of glacial erosional processes. Keiser et al. (2015) performed multivariate quantitative analysis in

the form of non-metric multidimensional scaling (NMDS) on sample sizes of ~30 grains to determine the possibility of glacial influence on grain micromorphology.

This study further expands quartz microtextural studies by systematically documenting quartz microtextures under double-blind conditions from modern fluvial systems in humid, arid, and glacial climatic settings to test the viability of using these microtextures as a paleoclimate indicator. However, this requires quantitative documentation of 1) microtextural occurrences unique to particular climates and 2) persistence of textures with some distance of fluvial transport.

If unique textures or suites of textures are found to be associated with a particular climate, then quartz microtextural analysis could become a viable tool to assess paleoclimatic conditions for deep-time fluvial strata in cases wherein quartz grains can be disaggregated effectively. This technique would be a valuable addition to paleoclimate studies on coarse-grained, first-cycle siliciclastic alluvial-fluvial strata, which commonly are climatically ambiguous. Discriminating between glacial and nonglacial alluvial sediment can be especially difficult, as such deposits exhibit many of the same facies characteristics (Williams and Rust, 1969; Church and Ryder, 1972; Miall, 1996). Glacially influenced deposits are particularly difficult to identify with confidence in the absence of clear ice-contact attributes (Dowdeswell et al., 1985; Eyles and Eyles, 1992); proglacial fluvial deposits appear very similar to coarse-grained alluvium formed in nonglacial settings (Miall, 1996; Bridge, 2006).

Finally, this study represents, to our knowledge, the first attempt of quartz microtextural data collection using a double-blind approach, wherein sample localities were obscured until completion of data collection. This approach guarded against any

inherent bias in texture recognition to provide a more robust test of the value of microtextural analysis.

Geological Background and Study Areas

Puerto Rico

Puerto Rico occupies the northern margin of the Caribbean Plate and is the smallest of the islands composing the Greater Antilles, with a land area of $\sim 9100 \text{ km}^2$ (Hayes et al., 1986; Schellekens, 1998; Pestle et al., 2013). Schellekens (1998) divided the igneous bedrock of the island into three provinces based on lithology, petrography, and geochemistry: the Central Igneous Province, the Southwestern Igneous Province, and the Northeastern Igneous Province. The San Lorenzo Batholith (Upper Cretaceous) underlies much of the Central Igneous Province and provides the primary source for most of the sediment sampled in this study (Hayes et al., 1985; Schellekens, 1998). Table 1 and Figure 1A detail the major lithologic types present.

Samples were collected along the Rio Guayanés in the municipality of Yabucoa in southeastern Puerto Rico. The mean annual precipitation (MAP; $\sim 2000 \text{ mm}$) and mean annual temperature (MAT; $26.5 \text{ }^\circ\text{C}$) designate this region as a tropical rainforest (Af on the Köppen climate classification; Southeast Regional Climate Center). The Rio Guayanés extends for $\sim 27 \text{ km}$ from its headwater region until its terminus at the marine shoreline. A major river, the Rio Guayabo, joins with the Rio Guayanés $\sim 12 \text{ km}$ from the headwater region. Six samples were collected along the first 15 km (Fig. 1A). Table 2 details key attributes of the transects. The Rio Guayanés drains a basin with an area of $\sim 44 \text{ km}^2$, and has an average downstream discharge of $\sim 1.67 \text{ m}^3/\text{s}$, and relief of 483 m (Díaz et al., 2005; USGS National Water Information System). Figure 2A illustrates a photograph of a sample site on the bank of the Rio Guayanés.

Norway

Norway forms part of the Paleozoic Caledonian belt and the modern Jotunheimen mountain chain. Within this chain, the Jostedalsgreen glacier complex covers $\sim 473.75 \text{ km}^2$, and is subdivided into glacier units based on drainage patterns, such as the Langedalsgreen and Austerdalsgreen alpine glaciers (Østrem and Haakensen, 1993; Andreassen et al., 2012) which, together with other glaciers of the Jostedalsgreen glacier complex, drain into fluvial and lacustrine systems (Sognefjorden in this study) that ultimately reach the Atlantic (Milnes et al., 1997). The major lithologic types underlying this region are granite, granodiorite and monzonite of Middle to Late Proterozoic age, variably affected by Caledonian-aged metamorphism to produce localized gneiss (Table 1 and Fig. 1; Lutro and Tveten, 1996; Skår and Pedersen, 2003).

Sediment samples were taken from a fluvial system near the town of Veitastrand, Norway. A MAP of $\sim 1100 \text{ mm}$ and MAT of $5.5 \text{ }^\circ\text{C}$ mark this system as continental subarctic (Dfc on the Köppen climate classification; climate-data.org). Three rivers occur in the study area: the river within Lange Valley (henceforth Lange River) heads at the Langedal Glacier, the river within Auster Valley (henceforth Auster River) heads at the Austerdal Glacier, and the Storelvi River emanates from the confluence of these two drainages. The Langedal Glacier and Austerdal Glacier form part of the larger aforementioned Jostedalsgreen glacier complex (Andreassen et al., 2012). The Lange River extends for $\sim 5 \text{ km}$ from the glacier terminus southeast to its confluence with the Auster River, and the Auster River extends for $\sim 7 \text{ km}$ from the glacier terminus southwest to the fluvial confluence. Following the merging of these

two rivers, the Storelvi River flows for ~9.5 km to its termination into Veitastrom Lake. Three samples were collected along the Auster River and four samples were collected along the Storelvi River (Fig. 1B). The Storelvi River has a drainage area of ~160 km², a discharge visually comparable to the Rio Guayanés, and a relief of 1625 m. Figure 2B shows the Storelvi River. Note the tributaries emanating from the sides of the valley.

Anza-Borrego, California

The Anza-Borrego Desert is located in southern California in the southwest United States and covers an area of ~2400 km². It is a subdivision of the larger Sonoran Desert, with bedrock comprising Cretaceous plutonic rocks ranging from gabbro to tonalite (Remeika and Lindsay, 1992). Tonalite makes up the entirety of the bedrock underlying the study location (Fig. 1C). Three major strike-slip fault systems (San Andreas, San Jacinto, and Elsinore) traverse the Anza-Borrego region (Dorsey et al., 2011), with the Elsinore Fault intersecting the studied transect (Fig. 1C).

Samples were collected along a fluvial system in Indian Gorge on the eastern face of the Tierra Blanca Mountains. The MAP of ~150 mm and MAT of ~22.6 °C mark this region as a desert (BWh on the Köppen climate classification; Western Regional Climate Center). The river sampled here is ephemeral (Fig. 2C), with active fluvial transport limited to times of heavy precipitation events. Indian Gorge has a drainage area of ~23 km² and a relief of 943 m. Samples were collected starting at the headwater through the beginning of the alluvial fan protruding from Indian Gorge. Five samples were collected along a ~7 km transect (Fig. 1C).

Peru

The sampling location is located in the Cordillera Blanca Batholith in the Ancash region of northern Peru (Fig. 2D). The Cordillera Blanca Batholith lies along the eastern border of the Rio Santa Basin, which formed associated with the Cordillera Blanca detachment fault, part of the larger Andean fold-thrust belt (Petford and Atherton, 1996; Giovanni et al., 2010). The mountains in this region range to 6.5 km elevation, sufficient to enable glaciation even in these tropical latitudes (Kaser et al., 2003; Suarez et al., 2008).

Sediment was collected near Yungay, Peru along the Rio Parón that emanates from proglacial Lake Parón, which in turn flows from the smaller Lake Artesón upstream. Figure 2D shows a photo of Lake Parón. The Rio Parón joins the Rio Santa river draining the Rio Santa Basin, fed primarily by $\sim 19 \text{ km}^2$ of glacial cover in the headwater regions (Kaser et al., 2003; Suarez, 2008). The sampling region within the Rio Santa drainage basin has an area of $\sim 85 \text{ km}^2$ and relief of $\sim 3356 \text{ m}$. Due to the large relief, the MAT and MAP vary considerably from the headwater to the most distal sampling point. The most proximal sampling location has a MAP of 787 mm (Kaser et al., 2003). Data from the nearest (10 km southeast) weather station (Llanganuco Valley), located at a comparable elevation to our proximal study location, records a MAT of $7.1 \text{ }^\circ\text{C}$ (Hellström and Mark, 2006). Thus, this region is cold semi-arid (BSk on the Köppen climate classification). In contrast, the distal sampling location near Caraz, a city along the Rio Parón $\sim 17 \text{ km}$ from Lake Parón, has a MAT of $15.5 \text{ }^\circ\text{C}$ and MAP of 252 mm, and thus characterized as a desert (BWk on the Köppen climate classification; climate-data.org). Two sediment samples were collected: the first at the terminus of

Lake Parón, and the second ~9 km down transect (Fig. 1D). The Cordillera Blanca fault bisects the Rio Parón approximately 1.7 km upstream of the distal sampling point.

Methods

Initial Research Design

Many factors influence physical and chemical attributes of siliciclastic sediment, including climate (e.g., Suttner et al., 1981; Johnsson et al., 1991; Cooke et al., 1993; Pye and Mazzullo, 1994; Pope et al., 1995, Anderson, 1997), bedrock composition/provenance (e.g., Nesbitt et al., 1996, 1997; White et al., 1999; Riebe et al., 2004), tectonic setting (Dickinson and Suczek, 1979; Dickinson and Valloni, 1980; Riebe et al., 2004), sediment environment and transport distance (Kairo et al., 1993), and drainage basin area and relief — both of which also co-vary with tectonic and climatic factors (Horton, 1945; Milliman and Syvitski, 1992; Leeder, 1993; Tucker and Slingerland, 1997; Whipple et al., 1999; Tucker, 2004). The siliciclastic sediment sampled as part of this study is from fluvial systems akin to alluvial strata preserved in the sedimentary record.

Sampled alluvial systems were chosen to represent both proglacial and nonglacial environments in climates subject to varied conditions of temperature and effective moisture, as follows: Puerto Rico represents a hot-humid, nonglacial system, Norway a cold-humid proglacial system, Peru a cold semi-arid to arid proglacial system, and California a hot-arid nonglacial system (Table 2). Other factors that influence siliciclastic sediment composition and weathering were controlled to the degree possible in an empirical study. For example, all sites are underlain by coarse-grained felsic to intermediate plutonic rock, with subordinate coarse-grained (gneissic) rock in Norway, and a minor contribution from metavolcanic rocks in Puerto Rico (detailed in Table 1 and Figure 1). Granitoids were chosen because they represent the

average composition of the upper continental crust (Rudnick and Gao, 2003), and granitoid weathering has been researched extensively in both natural and lab settings (White et al., 1999; Oliva et al., 2003; White and Brantley, 2003; Riebe, 2004). Tectonically, both the California and Peru localities represent active extensional settings, with the California locality traversed by the transtensional Elsinore Fault (Dorsey et al., 2011) and the Peru locality traversed by the Cordillera Blanca detachment fault (Petford and Atherton, 1996; Giovanni et al., 2010). Puerto Rico lies within an area of diffuse deformation linked to oblique strike-slip motion and extension associated with the boundary between the Caribbean and North American plates (Masson and Scanlon, 1991; Jansma and Mattioli, 2005). In contrast, Norway is tectonically passive relative to the other locations in this study, although has experienced recent uplift associated with post-glacial isostatic rebound (Lidmar-Bergström et al., 2000). All sites were sampled beginning from the proximal-most point (headwaters region, glacial terminus, or proglacial lake) and extending downstream for 7-15 km (Table 2). All sites were chosen to target comparable drainage basin size and relief, albeit these values do vary by factors of ~2-7, owing to the complexities of natural systems (Table 2).

Field Sampling

For all study sites, first-cycle sediment samples, including mud-, sand-, and gravel-sized material, were collected from slack-water areas of lateral bars with a clean hand trowel. Samples were collected at intervals along fluvial system transects in Puerto Rico, Norway, California, and Peru, beginning at the headwater regions of each fluvial system and proceeding downstream (Table 2). The Peruvian fieldwork was completed

after data collection for the samples from Norway, California, and Puerto Rico. Due to time constraints, only two locations (thus fewer grains) were analyzed from Peru: near the proglacial lake (proximal) and 9 km down transect (distal). Samples were kept in frozen storage until processing (detailed below).

Laboratory Processing

Following previous studies, the medium- to coarse-grained sand fraction (250 μm to 1 mm) was selected for this study. A large grain-size range should show a larger range of textures, as different textures can be more or less prevalent depending on grain size (Krinsley and Smith, 1981; Mahaney, 2002). The sand was isolated by gently wet sieving the bulk sample. The sieved sand was then treated with 30% hydrogen peroxide (H_2O_2) at 50 °C for 24 hours to remove organic matter, and then rinsed thoroughly. The samples were then treated with 1N hydrochloric acid (HCl) at 50 °C for 24 hours to remove any carbonate coatings; previous tests have shown that low HCl concentrations at these temperatures and timeframes do not influence quartz microtextures, as demonstrated by before-and-after tests (Pye, 1983; Keiser et al., 2015). Finally, the samples were treated using the citrate-bicarbonate-dithionite (CBD) method (Rea and Janecek, 1981) to remove iron-oxide and manganese-oxide coatings, and rinsed. The grains were not sonicated, in order to prevent artificially inducing microtextures (Porter, 1962).

Following the treatment steps, individual quartz grains were randomly selected by visual examination using a reflected-light microscope following the method of Mahaney et al. (1988), mounted on an aluminum stub with double-sided carbon tape, and sputter coated with a gold-palladium mixture to prevent charging for SEM analysis.

Each stub held ~28 grains, arranged in rows to enable unique identification of each grain, and prevention of duplicate analysis of the same grain (Fig. 3). Two stubs (~50 grains) were analyzed for each sample location along the transect.

For SEM analysis, a FEI Quanta Scanning Electron Microscope was used in secondary electron mode with the following settings: a spot size of 5 (dimensionless), a working distance of 10 mm, and an accelerating voltage of 20 kV. Each grain was also analyzed with energy-dispersive X-ray spectroscopy (EDS) to confirm quartz mineralogy of the grains prior to microtextural analysis.

Previous studies have advocated varied approaches regarding the number of grains suitable for analysis, and no single universal sample size has been accepted (Bull, 1981; Mahaney, 2002). Table 3 summarizes the parameters (number of grains, and size fractions) employed by a selection of previous studies and notes the sample size and size fraction for each study. Sample sizes range from 10 to >100 grains, and size fractions analyzed range from 63 μm to 3 mm. Mahaney (2002) suggested examination of a minimum of 20 grains from both the medium-grained sand fraction (250 μm to 500 μm) and the coarse- to very coarse-grained sand fraction (500 μm to 2 mm), although the aims of the study should ultimately dictate the number of grains analyzed. Deane (2010) suggested the examination of at least 100 grains for performing statistical analyses, whereas Costa et al. (2012) advocated a median number of 20 grains per sample for statistical analyses. For this project, ~50 grains per sample were analyzed. The size range selected for analysis (250 μm - 1 mm) encompasses the size fractions most easily transported in saltation in unidirectional flow.

A spreadsheet was created (Appendix C) to record the presence/absence of the microtextures for every grain. There were 40 stubs analyzed from 20 sample sites, with a total of ~50 grains per site. To ensure objective analysis, SEM microtextural “scoring” was conducted by the same operator (Smith), in a double-blind manner wherein sample identifications (and thus site localities) were kept concealed until completion of all data collection, with the exception of the Peruvian samples. A total of 993 quartz grains (Puerto Rico—297; Norway—346; California—250; Peru—100) were scored for the presence or absence of 17 microtextures (Table 4), along with the degree of roundness and relief for each grain. Each microtexture was recorded as being either present or absent in the style of Mahaney (2002). No estimation of coverage or spatial relationship between or within textures was made.

Principal Component Analysis

For quantitative analysis, principal component analysis (PCA) was performed. The goal of PCA is to determine a new set of variables (principal components) and prioritize those variables in order of their statistical variance to ultimately reduce the number of variables needed to explain the majority of variance in the data. These principal components are linearly uncorrelated, and used as x and y axes on which the original multidimensional data can be plotted in two dimensions. The number of principal components equals the number of variables in the original data set; however, not all of the derived principal components contain enough variance to describe a significant portion of the data; those that fail to describe a significant part of the data are disregarded, resulting in data reduction.

If the original set of data is plotted onto multidimensional space, PCA deconstructs the data into eigenvectors and eigenvalues. Eigenvectors are vectors that describe variance in the data and, importantly, do not change direction with linear transformation. For every eigenvector, a corresponding eigenvalue exists that is scaled through the linear transformation process, and describes the magnitude of the eigenvector. PCA calculates eigenvectors, now termed principal components, and prioritizes them based on their ability to describe variance in the data. The first principal component bisects the data and explains the most variance, the second principal component is orthogonal to the first and explains the second amount of variance, and each subsequent principal component explains a decreasing amount of variance while maintaining orthogonality to the first principal component.

Each principal component correlates to the original variables through “loadings,” wherein each of the variables is assigned a loading score (-1 to 1) that describes its correlation to each component. Loadings are inherently related to eigenvectors and eigenvalues as loadings are the product of the square root of an eigenvalue and its corresponding eigenvector. The more positive a loading score, the more positive the correlation between a variable and principal component; in contrast, a negative score indicates a negative correlation. Significant loading values are selected based on their scores relative to the scores of the other variables. Data are then plotted on scatter plots wherein the x and y axes equate to the principal components, and data points plot based on their relationship to only those principal components. This enables visualization of data behavior under the influence of only those variables accounting for the most variance, while eliminating variables that PCA determines to be insignificant. To

summarize, loadings are the correlations between the original variables and the new unit-scaled principal components. For example, when a data point (sediment sample location) has a high positive score for a principal component, those variables (microtextures) that have high positive loadings for that principal component exert a large influence on that data point.

The raw data for this study were validated for potential PCA by converting the nominal-scale data (absence/presence binary values) into ratio-scale data by averaging the scores of each microtexture for each of the 40 samples analyzed using the aforementioned method. Subsequently, PCA was run on the variance-covariance matrix. Statistical analysis was completed in Microsoft Excel and Paleontological Statistics (PAST) v. 3.11 (Hammer and Dat, 2001).

Results of Microtexture Analysis

Univariate Location Results

Overall, the most common microtextures encountered are dissolution etching and conchoidal fractures occurring on 82% and 73% of the grains, respectively (Figs. 3, 4). The least common textures are straight grooves, curved grooves, and deep troughs, occurring on 4%, 3%, and 2% of the grains, respectively. The samples from Puerto Rico display a much higher incidence of precipitation features at 61%, compared to 37% in Norway, 30% in California, and 27% in Peru. Samples from both Peru and Norway exhibit a higher percentage of fracture faces (18% and 12%, respectively) relative to those from Puerto Rico (4%) and California (6%). The Norway samples exhibit the highest concentration of both arc-shaped steps (54%) and linear steps (66%), whereas California samples exhibit 52% arc-shaped steps and 54% linear steps, Puerto Rico samples exhibit 46% arc-shaped steps and 53% linear steps, and Peru samples contain 38% arc-shaped steps and 49% linear steps. Samples from California and Peru show higher percentages of upturned plates (44% and 42%, respectively) compared to those from Puerto Rico (35%) and Norway (26%). Lastly, Peru displays the highest occurrence of subparallel linear fractures (77%). See Table 5 for the occurrence of each texture per location and Appendix A for raw microtexture counts.

Percussion-induced textures (v-shaped percussion cracks and edge rounding) were plotted (Fig. 5) to illustrate occurrence versus sampling location for each transect. Only the Peruvian samples exhibit a trend — an increase in incidence of both textures from proximal to distal localities.

Principal Component Analysis

Principal component analysis was performed in two ways: the first consisting of all 17 microtextures, both chemically and mechanically induced, and the second consisting of only the 15 mechanically induced microtextures. Table 6 provides a summary of the principal components chosen for each of the data sets. Analysis of each data set resulted in a set of plots that illustrates the relationship of each variable (microtexture) on each principal component, and a corresponding graph that shows the position of each sediment sample relative to each principal component.

All Textures

The first three principal components were chosen for the first PCA run (utilizing all microtextures) as they account for >62% of the total variation (Table 6). Precipitation features score the highest for the first principal component (PC1), suggesting that this microtexture exerts the largest influence on data segregation. Incidence of upturned plates account for the largest positive loading for PC2, whereas conchoidal fractures contribute the largest negative loading value. Lastly, linear steps score the largest loading value for PC3, although high positive loadings also occur for selected other textures (arc-shaped steps, dissolution etching, and v-shaped cracks) that could obscure the influence of linear steps. However, one variable—upturned plates—exhibits a negative loading score higher than the others. See Table 7 for detailed loading values and Figures 6A and 6C for correlations between the microtextures and the principal components.

When the first data set (containing all textures) is projected onto PC1 and PC2 (x- and y-axes respectively; Fig. 6B), the majority of the Puerto Rico samples are

differentiated from the other sample sets by their high PC1 scores, wherein a positive PC1 score mostly reflects a measure of precipitation features. This projection also reveals that the more distal Puerto Rico samples have increasingly less positive PC1 scores, suggesting a loss of influence of precipitation features as these grains move farther from the headwaters. The Puerto Rico samples exhibit a large variance relative to their PC2 scores, suggesting that variables associated with PC2 are not especially useful for discriminating Puerto Rico samples from other data sets. A majority of California samples exhibit high PC2 scores, mostly reflecting the influence of upturned plates, but display a large range of PC1 scores. The Norway samples exhibit a range of low negative scores to moderate negative scores with PC2, suggesting a greater occurrence of conchoidal fractures relative to upturned plates, together with near-zero to negative PC1 scores, indicating a low incidence of precipitation features. Lastly, the Peru samples exhibit high negative scores with PC1, suggesting a low incidence of precipitation features. The Peruvian samples also display near-zero PC2 scores, indicating either no significant influence (negative or positive) of conchoidal fractures or upturned plates, or high incidence of upturned plates counterbalanced by high incidence of conchoidal fractures. The second is more likely as univariate analysis already showed that the Peru data set exhibits a high average amount of upturned plates and conchoidal fractures.

Figure 6D projects the data onto PC1 and PC3. Again, the Puerto Rico data set has the highest scores for PC1. Puerto Rico exhibits a large range of scores for PC3, suggesting those variables that contribute high loadings to PC3 are less useful for discriminating the Puerto Rico data set. The California data set has consistent negative

scores for PC3, suggesting a higher incidence of upturned plates. The Peru samples have the highest negative scores for PC3, suggesting that these samples also exhibit a high incidence of upturned plates. Lastly, the Norway samples exhibit near-zero to positive scores for PC3 suggesting a high influence of linear steps, arc-shaped steps, dissolution etching, and v-shaped cracks. However, the equally high scores of multiple variables that exert positive loading values for PC3 causes ambiguity in distinguishing which exhibits the highest influence on the Norway samples.

Mechanical Textures

The second PCA run assessed only mechanical textures, and here the first three components capture >62% of the total variation in the data (Table 6). Occurrence of upturned plates contributes the largest positive loading for PC1, whereas incidence of conchoidal fractures contributes the largest negative loading score. Both arc-shaped steps and linear steps have significant positive loading values for PC2. V-shaped cracks exhibit a large negative score for PC3, whereas upturned plates exhibit the largest positive loading score. The significant loading values for arc-shaped and linear steps suggest that these textures tend to co-occur. See Table 8 for more detail on the loading values and Figure 7 for correlations between microtextures and principal components.

Figure 7B shows the data projected onto PC1 and PC2. The majority of the Norway data set exhibits large positive scores for PC2, indicating a large influence of linear and arc-shaped steps, with the exception of the NOR2 sample. The Norway set also has consistent negative PC1 scores, indicating low incidence of upturned plates and high incidence of conchoidal fractures. Both the California and Puerto Rico samples display a range of scores for PC1, suggesting that some samples have a higher

proportion of upturned plates, whereas others have a higher proportion of conchoidal fractures. Both of these sets also exhibit a range of PC2 scores, recording a variable influence of arc-shaped steps and linear steps. Lastly, both Peruvian samples have near-zero PC1 scores and negative PC2 scores, suggesting a large influence emanating from a lack of steps, and large incidences of both upturned plated and conchoidal fractures.

Figure 7D shows the sample points projected onto PC1 and PC3. The Puerto Rico samples exhibit negative PC3 scores, indicating a higher occurrence of v-shaped cracks and lower occurrence of upturned plates. California samples exhibit both high PC1 and PC3 scores, suggesting high amounts of upturned plates. The Peru samples have near-zero scores for PC1, and high positive scores for PC3, indicating a high incidence of upturned plates and a low incidence of v-shaped cracks.

Summary

PCA results suggest that the largest source of discrimination results from the occurrence of precipitation features in the Puerto Rico samples in the first PCA run. Analyses from both PCA runs indicate that the Peru samples contain a high incidence of upturned plates and conchoidal fractures; however, conchoidal fractures are not unique to this location. Upturned plates are also common in the samples from California. Samples from Norway have a lower incidence of upturned plates and higher incidence of conchoidal fractures, although not significantly different from the other locations. Samples from Puerto Rico contain the highest incidence of v-shaped cracks, followed by the Norway samples. Additionally, textures not considered significant by PCA suggests that they do not impart sufficient variance in the data to be useful for distinguishing samples from the different localities. Lastly, univariate analysis

demonstrates that fracture faces occur more commonly in the samples from Peru and Norway.

Ternary Analysis

Combining the PCA results that identified those textures accounting for the greatest variance (differentiation) among the sample sets, along with results from univariate analysis, enabled identification of a subset of textures that account for the largest distinction among the study locations. These textures were then used as the apices for a ternary plot: 1) upturned plates 2) fracture faces and subparallel linear fractures 3) precipitation features and v-shaped cracks (Fig. 8). The Puerto Rico samples plot nearer to the apex with precipitation features and v-shaped cracks. Both the California and Peru samples trend toward the upturned plates apex, although the California data set demonstrates large intrasample variability. The Peru samples trend toward the subparallel linear fracture apex, whereas the Norway and Peru samples trend toward the apex representing fracture faces and subparallel linear fractures.

Discussion

Comparisons with Previous Studies

Results from our study exhibit both similarities to and differences from previous microtextural studies. For example, the large incidences of chemical features (precipitation features and dissolution etching) reported in the tropical Puerto Rico grains are similarly reported by Doornkamp and Krinsley (1971), who suggested that chemical features are the most diagnostic textures for tropical environments. Doornkamp (1974) documented both precipitation and dissolution features on detrital quartz originating from weathered granite from England where precipitation levels (2000 mm MAP) are comparable to those in Puerto Rico, and suggested that pervasive soil water in this climate leads to common silica precipitation.

In contrast, our results differ somewhat from published results on grains from glacial/proglacial environments. Mahaney and Kalm (2000) documented subparallel linear fractures, conchoidal fractures, v-shaped percussion fractures, and edge rounding on glaciofluvial sands. Similar to the proglacial samples reported in Mahaney and Kalm (2000), proglacial fluvial samples from Norway and Peru exhibit very low instances of curved grooves, straight grooves, and troughs, possibly indicating that glacial textures are rapidly overprinted upon entering the fluvial system; however, the grains from all four locations (both proglacial and nonglacial) studied here exhibit comparatively high incidences of crescentic gouges, steps (both arc-shaped and linear), and conchoidal fracturing. Other studies have found much higher occurrences of deep troughs, curved grooves, and straight grooves on deposits of glacial origin than were found in this study (Deane, 2010; Strand and Immonen, 2010; Sweet and Soreghan 2010; Woronko, 2016).

These features in particular are considered as possible “microstriae” attributable to a “stylus” effect, thought to form in a manner akin to macroscopic striations taken as quintessential indicators of glacial abrasion (Mahaney, 2002).

Crescentic gouges have also been assumed as glaciogenic, although previously published results vary regarding the occurrence of this microtexture in glacial settings. Analogous to macroscopic striae, macroscopic crescentic gouges have long been associated with glaciation (e.g., Gilbert, 1906; Benn and Evans, 1998). Rose and Hart (2008), for example, reported a 20-70% occurrence of (microscopic) crescentic gouges in sediments from modern glacial samples. In contrast, Mahaney (2002) suggested that the utility of this feature is limited owing to its rarity ($\ll 1\%$ occurrence). Woronko (2016) similarly reported an absence of microscopic crescentic gouges on grains from glacial diamicton. We report occurrences ranging from 16%-22% across all climates represented, calling into question an exclusive glaciogenic origin for this microtexture.

Additionally, many authors have associated the occurrence of arc-shaped steps (and to a smaller extent, linear steps) with glacial environments (Krinsley and Doornkamp, 1973; Higgs, 1979; Mahaney and Kalm, 2000; Mahaney, 2002; Deane, 2010; Immonen, 2013; Vos et al., 2014). In the present study, the Norway (proglacial) grains exhibit a higher percentage of linear- and arc-shaped steps than other localities, but the Peru (proglacial) grains displayed the lowest count for both types of steps. These findings call into question a possible glacial causation for both linear- and arc-shaped steps and suggest that other (non-glacial) processes contribute to the formation of these microtextures as well.

Finally, many previous studies have linked formation of subparallel linear fractures to glaciogenic processes (Krinsley and Doornkamp, 1973; Mahaney and Kalm, 2000; Deane, 2010; Immonen, 2013; Vos et al., 2014; Woronko, 2016). Results from the Peru (proglacial) samples seemingly corroborate this, as they contain the highest incidence (77%) of subparallel linear fractures of all localities in this study. However, the Norway (proglacial) samples exhibit the same incidence of subparallel linear fractures as the California (nonglacial) samples (both 68%), refuting an exclusively glacial origin for this texture. This result is consistent with Mahaney (2002), who suggested that high amounts of subparallel linear fractures are generally common in large sample sets.

Application of Quartz Microtextures as a Climate Proxy

The results from PCA and derivative ternary plots suggest that grains from the various study locations can be distinguished, albeit to varying degrees, and with relatively subtle distinctions. Moreover, no significant trends occur in the evolution of textures with the transport distances (7-15 km) assessed in this study, with the exception of the Puerto Rico grains, which exhibit loss of precipitation features with transport distance. This persistence of textures indicates the potential for preservation of weathering-induced microtextures in proximal fluvial systems of the sedimentary record.

The ternary diagram (Fig. 8) serves to illustrate the trends between and within sample locations. The apices chosen (on the basis of PCA results) enable the best discrimination among sample sets. The samples from California display the largest intersample variance, whereas the samples from Puerto Rico and Norway cluster most

tightly. The most statistically robust distinction separates the arid (California and Peru) and humid (Puerto Rico and Norway) locations, and this distinction is most clear among samples from the most proximal locations. The arid locations consistently trend closer to the upturned apex than do the humid locations, whereas the humid locations trend toward the apex representing precipitation features and v-shaped cracks. A more subtle distinction occurs between the glacial (Peru and Norway) and nonglacial (Puerto Rico and California) samples, wherein glacial samples trend toward the apex characterized by the occurrence of fracture faces and subparallel linear fractures.

The increased incidence of precipitation features in the humid data set is accompanied by a larger occurrence of dissolution etching. This result likely reflects the intense chemical weathering potential in Puerto Rico, where both high precipitation and high temperatures (Table 2) lead to formation of a thick regolith in a transport-limited setting. White et al. (1998) characterized regolith formation in eastern Puerto Rico and described increased silica concentration in pore waters with depth (1 to 4 m), indicating a greater potential for silica precipitation with depth. Quartz grains exhibiting silica precipitation then enter the fluvial system primarily via mass wasting from the relatively high-relief hillsides. The decreasing incidence of precipitation features with downstream transport reinforces the interpretation that silica precipitation occurs during regolith formation, before introduction of the grains into the fluvial system. Although the incidence of precipitation features decreases with downstream transport, it nevertheless remains sufficiently high to enable differentiation of this data set from all others. The Norway samples exhibit the second highest occurrences of both precipitation and dissolution features, interpreted to similarly reflect the significant

influence of water-rock interaction in this humid and highly vegetated environment. Here, quartz grains entering the stream system likely emanate from both the subglacial system and the highly vegetated cut banks of the stream system. Slope failure along cut banks in this system reveal older alluvial deposits beneath a layer of peat. Hence, we infer that, despite the cold temperatures, the overall humidity and associated vegetation along the stream system, as well as the perennially wet subglacial environment in this temperate glacial setting promote weathering sufficient to effect silica precipitation and dissolution features. Additionally, freeze-thaw cycles have been suggested to cause silica precipitation (Dietzel, 2005; Woronko, 2016).

In contrast to the humid-climate fluvial systems, quartz grains from both arid environments (California and Peru) exhibit substantially lower incidences of precipitation features and slightly lower amounts of dissolution etching, consistent with the substantially more arid settings. Additionally, samples from both the California and Peru localities exhibit the highest incidences of upturned plates. Upturned plates have been considered a high-stress fracture in some previous studies owing to the inferred formation processes, which include aeolian transportation and neotectonic processes. Both the California and Peru localities are characterized by (varying degrees of) aridity (leading to potential aeolian transportation) and also transect active fault systems. Although Mahaney (2002) suggested that upturned plates could reflect rapid grain breakage during faulting, no significant differences occur in incidences of upturned plates upstream and downstream of the faulting in both the California and Peru localities. However, upturned plates have also been documented on quartz grains subjected to aeolian transport in both natural and laboratory studies (Wellendorf and

Krinsley, 1980; Mahaney, 2002; Marshall et al., 2012; Costa et al., 2013). The California locality represents an ephemeral alluvial setting subject to intermittent aeolian activity; the Rio Parón (Peru) exhibits perennial flow, but this system transits arid regions both proximally (the high-elevation glacial headwaters) and distally (in the increasingly arid lower-elevation region). Thus, both fluvial systems transit arid regions that could allow the introduction of aeolian-influenced sand into their systems.

The two glacial locations (Peru and Norway) can be distinguished from the other regions by the higher occurrences of fracture faces, although these microtextures have been previously associated with dislodgement from crystalline source rock and not necessarily glacial processes (Krinsley and Doornkamp, 1973; Higgs, 1979; Mahaney, 2002). However, Woronko (2016) reported high incidences of fracture faces (~50%) in glacial diamicton. Schwamborn et al. (2012) and Woronko (2016) suggested that fracture faces can also result from freeze-thaw cycles common in periglacial settings.

Complexity of Natural Systems

Natural systems are expected to exhibit inherent complexity in microtextural attributes, as it is difficult to control for all variables that could affect weathering, and the climate of each locality varies in both temperature and precipitation space. This variability can obfuscate trends, as well expressed in ternary space (Fig. 8), as every location exhibits some intersample spread. Additionally, there seem to be few trends as the grains move down the transect. This lack of downstream trends may in part reflect the influence of tributaries, which contribute sediment exposed to varying degrees of chemical and physical weathering. Furthermore, time averaging of the climate signal occurs in any system as a channel cannibalizes older fluvial deposits deposited in

slightly different climatic conditions, and/or subject to a longer residence time in (potentially vegetated) interfluves, etc.

Figure 9 schematically illustrates the complexity associated with the climatic settings of the studied systems. As illustrated, these localities overlap in both precipitation and temperature space, and in the presence or absence of a glacial influence. This multidimensional overlap helps to explain the complexity of the microtextural signal, and the difficulty associated with clearly differentiating these climate extremes. Nevertheless, use of PCA to identify the most distinctive microtextures of each locality demonstrates that textures or suites of textures do effectively enable differentiation of these climatic settings.

Methodological Recommendations

There have been varied approaches to conducting previous SEM microtextural studies, especially regarding methods for data recording, number of grains to analyze, and use of qualitative and quantitative analysis techniques. The double-blind approach on modern systems taken in this study has led to the following recommendations to aid in future analyses.

1) To the extent possible, double-blind conditions, with analyses conducted by a single operator, should be employed to guard against any inherent biases. Microtextural recognition is somewhat qualitative, so a double-blind approach helps to minimize biased recognition of textures that “should” be present.

2) The historically used binary “presence vs. absence” approach may prove inferior to an approach that considers percent coverage of microtextures on a single grain. This is especially important for common textures that cover highly variable

amounts of surface area, such as precipitation features, dissolution etching, and v-shaped percussion cracks. In the “presence vs. absence” approach, a single v-shaped percussion crack, for example, is rated as equally important as a grain exhibiting full surface coverage by many percussion cracks.

3) Although histograms for data display are traditionally used (e.g. Campbell and Thompson, 1991; Mahaney and Kalm, 2000; Mahaney, 2002), they are less visually useful than ternary plots (cf. Sweet and Soreghan, 2010; Keiser et al., 2015). However, the apices used in such ternary plots should be determined by quantitative statistical analyses of the raw data.

4) Many different approaches have been taken regarding the number of grains analyzed, as demonstrated in Table 3. Examination of the 50 grains per sampling location in this study provided adequate numbers for statistical analysis, along with providing enough resolution to pick up the microtextures that occurred in the lowest numbers, specifically microstriae. However, more grains analyzed should enable better discrimination.

Conclusions

This study focused on the application of quartz microtextural analyses to assess climatically influenced weathering from modern fluvial systems representing “endmember” precipitation and temperature states, including both proglacial and nonglacial systems. Selection of study regions to minimize differential influences of non-climatic factors (bedrock lithology, drainage basin size, transport distance), use of a double-blind approach for data collection, and quantitative analysis of results were employed to test whether microtextural attributes enable distinction of grains from different climates. Results indicate that samples from Puerto Rico (hot-humid climate) are dominated by precipitation features and v-shaped percussion cracks, with precipitation features also common in humid Norway (cold-humid proglacial). Precipitation features are interpreted to reflect the influence of sustained water-rock interaction in these humid climates. Samples from both arid locations (California and Peru) exhibit higher incidences of upturned plates, attributable in part to high-stress eolian impacts in these environments. Finally, samples from proglacial systems (Norway and Peru) exhibit a much higher incidence of fracture faces and a (less pronounced) increase in occurrence of subparallel linear fractures relative to the hot-humid location, interpreted to reflect the actions of glacial crushing and freeze-thaw weathering, respectively.

These results, combined with results from Sweet and Soreghan (2010), which illustrated that microtextures remain recognizable even in lithified deep-time deposits subjected to diagenetic overprinting, suggest that SEM microtextural studies can be a

viable paleoclimate proxy. However, the signal can be complex, in part because climate states are characterized by variation in multiple parameters (precipitation, temperature, nonglacial, glacial), with potential overlap of sets of variables. Furthermore, factors such as time averaging, natural variability of source lithology, and drainage basin size could further complicate signals. We suggest that future studies adopt a double-blind and quantitative statistical approach to help reduce the effects of an inherently qualitative scoring process.

References Cited

- Anderson, S.P., Drever, J.I., and Humphrey, N.F., 1997, Chemical weathering in glacial environments: *Geology*, v. 25, p. 399–402.
- Andreassen, L.M., Winsvold, S.H., Paul, F., Hausberg, J.E., 2012. Inventory of Norwegian glaciers: Norwegian Water Resources and Energy Directorate, v. 38, 236 p.
- Armstrong-Altrin, J.S., and Natalhy-Pineda, O., 2014, Microtextures of detrital sand grains from the Tecolutla, Nautla, and Veracruz beaches, western Gulf of Mexico, Mexico: Implications for depositional environment and paleoclimate: *Arabian Journal of Geosciences*, v. 7, p. 4321–4333.
- Benn, D.I., and Evans, D.J.A., 1998, *Glaciers and Glaciation*: London, U.K., Arnold Publishers, 734 p.
- Biederman Jr, E.W., 1962, Distinction of shoreline environments in New Jersey: *Journal of Sedimentary Research*, v. 32, p. 181–200.
- Blott, S.J., and Pye, K., 2007, Particle shape: A review and new methods of characterization and classification: *Sedimentology*, v. 55, p. 31-63.
- Bridge, J.S., 2006, Fluvial facies models: Recent developments, in Posamentier, H.W., and Walker, R.G., eds., *Facies models revisited: SEPM (Society for Sedimentary Geology) Special Publication 84*, p. 85–170.
- Brown, J.E., 1973, Depositional histories of sand grains from surface textures: *Nature*, v. 242, p. 396–398.
- Bull, P.A., 1981, Environmental reconstruction by electron microscopy: *Progress in Physical Geography*, v. 5, p. 368–397.

- Campbell, S., and Thompson, I.C., 1991, The palaeoenvironmental history of Late Pleistocene deposits at Moel Tryfan, North Wales: Evidence from scanning electron microscopy (SEM): *Proceedings of the Geologists' Association*, v. 102, p. 123–134.
- Chakroun, A., Miskovsky, J.-C., and Zaghib-Turki, D., 2009, Quartz grain surface features in environmental determination of aeolian Quaternary deposits in northeastern Tunisia: *Mineralogical Magazine*, v. 73, p. 607–614.
- Church, M., and Ryder, J.M., 1972, Paraglacial sedimentation: a consideration of fluvial processes conditioned by glaciation: *Geological Society of America Bulletin*, v. 83, p. 3059–3072.
- Clinkenbeard, J.P., and Walawender, M.J., 1989, Mineralogy of the La Posta Pluton; implications for the origin of zoned plutons in the eastern Peninsular Ranges Batholith, Southern and Baja California: *American Mineralogist*, v. 74, p. 1258–1269.
- Cooke, R.U., Warren, A., Goudie, A.S., 1993. *Desert Geomorphology*. University College London Press, London.
- Costa, P.J.M., Andrade, C., Dawson, A.G., Mahaney, W.C., Freitas, M.C., Paris, R., and Taborda, R., 2012, Microtextural characteristics of quartz grains transported and deposited by tsunamis and storms: *Sedimentary Geology*, v. 275–276, p. 55–69.
- Costa, P.J.M., Andrade, C., Mahaney, W.C., Marques da Silva, F., Freire, P., Freitas, M.C., Janardo, C., Oliveira, M.A., Silva, T., and Lopes, V., 2013, Aeolian

- microtextures in silica spheres induced in a wind tunnel experiment:
Comparison with aeolian quartz: *Geomorphology*, v. 180-181, p. 120–129.
- Deane, S.M., 2010, Quartz grain microtextures and sediment provenance: Using scanning electron microscopy to characterize tropical highland sediments from Costa Rica and the Dominican Republic [M.S. thesis]: University of Tennessee, Knoxville, Tennessee, 123 p.
- Díaz, P.L., Aquino, Z., Figueroa-Álamo, C., García, R., and Sánchez, A.V., 2005, Water resources data Puerto Rico and the U. S. Virgin Islands water year 2003: U. S. Geological Survey, Water Data Report PR-00-1, 698 p.
- Dickinson, W.R., and Suczek, C.A., 1979, Plate tectonics and sandstone compositions: *American Association of Petroleum Geologists Bulletin*, v. 63, p. 2164–2182.
- Dickinson, W.R., and Valloni, R., 1980, Plate settings and provenance of sands in modern ocean basins: *Geology*, v. 8, p. 82–86.
- Dietzel, M., 2005, Impact of cyclic freezing on precipitation of silica in Me–SiO₂–H₂O systems and geochemical implications for cryosoils and -sediments: *Chemical Geology*, v. 216, p. 79–88.
- Doornkamp, J.C., 1974, Tropical weathering and the ultra-microscopic characteristics of regolith quartz on Dartmoor: *Geografiska Annaler. Series A, Physical Geography*, v. 56, p. 73.
- Doornkamp, J.C., and Krinsley, D.H., 1971, Electron microscopy applied to quartz grains from a tropical environment: *Sedimentology*, v. 17, p. 89-101.
- Dorsey, R.J., Housen, B.A., Janecke, S.U., Fanning, C.M., and Spears, A.L., 2011, Stratigraphic record of basin development within the San Andreas fault system:

- Late Cenozoic Fish Creek–Vallecito basin, southern California: Geological Society of America Bulletin, v. 123, p. 771–793.
- Dowdeswell, J.A., Osterman, L.E., and Andrews, J.T., 1985, Quartz sand grain shape and other criteria used to distinguish glacial and non-glacial events in a marine core from Frobisher Bay, Baffin Island, NWT, Canada: Sedimentology, v. 32, p. 119–132.
- Eyles, N., and Eyles, C. H., 1992, Glacial depositional systems, in Walker, R. G., ed., Facies models: Response to sea-level change: Geological Association of Canada, p. 73–100.
- Giovanni, M.K., Horton, B.K., Garziona, C.N., McNulty, B., and Grove, M., 2010, Extensional basin evolution in the Cordillera Blanca, Peru: Stratigraphic and isotopic records of detachment faulting and orogenic collapse in the Andean hinterland: Tectonics, v. 29, p. 1–21.
- Gilbert, G.K., 1906, Crescentic gouges on glaciated surfaces: Geological Society of America Bulletin, v. 17, p. 303–316.
- Gomez, B., and Small, R.J., 1983, Genesis of englacial debris within the lower Glacier de Tsidjiore Nouve, Valais, Switzerland, as revealed by scanning electron microscopy: Geografiska Annaler. Series A, Physical Geography, v. 65, p. 45–51.
- Hammer, H., and Dat, R., 2001, PAST: paleontological statistics software package for education and data analysis: Palaeontology Electron 4: <http://palaeo-electronica.org/2011/past/issue101.htm>.

- Hayes, J.A., Larue, D.K., Joyce, J., and Schellekens, J.H., 1986, Puerto Rico: reconnaissance study of the maturation and source rock potential of an oceanic arc involved in a collision: *Marine and Petroleum Geology*, v. 3, p. 126–138.
- Helland, P.E., Huang, P.-H., and Diffendal Jr, R.F., 1997, SEM analysis of quartz sand grain surface textures indicates alluvial/colluvial origin of the Quaternary “glacial” boulder clays at Huangshan (Yellow Mountain), East-Central China: *Quaternary Research*, v. 48, p. 177–186.
- Hellström, R. Å, and Mark, B.G., 2006, An embedded sensor network for measuring hydrometeorological variability within an alpine valley, *in* 63rd Eastern Snow Conference, Newark, Delaware, p. 263–297.
- Higgs, R., 1979, Quartz-grain surface features of Mesozoic-Cenozoic sand from the Labrador and western Greenland continental margins: *Journal of Sedimentary Geology*, v. 49, no. 2, p. 599-610.
- Horton, R.E., 1945, Erosional development of streams and their drainage basins; hydrophysical approach to quantitative morphology: *Geological Society of America Bulletin*, v. 56, p. 275–370.
- Immonen, N., 2013, Surface microtextures of ice-rafted quartz grains revealing glacial ice in the Cenozoic Arctic: *Palaeogeography, Palaeoclimatology, Palaeoecology*, v. 374, p. 293–302.
- Jansma, P.E., and Mattioli, G.S., 2005, GPS results from Puerto Rico and the Virgin Islands: Constraints on tectonic setting and rates of active faulting: *in* Mann, P., ed., *Active Tectonics and Seismic Hazards of Puerto Rico, the Virgin Islands, and Offshore Areas*: Geological Society of America Special Paper 385, p.13-30.

- Johnsson, M.J., Stallard, R.F., and Lundberg, N., 1991, Controls on the composition of fluvial sands from a tropical weathering environment: Sands of the Orinoco River drainage basin, Venezuela and Colombia: *Geological Society of America Bulletin*, v. 103, p. 1622–1647.
- Kairo, S., Suttner, L.J., And Dutta, P.K., 1993, Variability in sandstone composition as a function of depositional environment in coarse-grained delta systems, in Johnsson, M.J., and Basu, A., eds., *Processes Controlling the Composition of Clastic Sediments: Geological Society of America, Special Paper 284*, p. 263–283.
- Kaser, G., Juen, I., Georges, C., Gómez, J., and Tamayo, W., 2003, The impact of glaciers on the runoff and the reconstruction of mass balance history from hydrological data in the tropical Cordillera Blanca, Perú: *Journal of Hydrology*, v. 282, p. 130–144.
- Keiser, L.J., Soreghan, G.S., and Kowalewski, M., 2015, Use of quartz microtextural analysis to assess possible proglacial deposition for the Pennsylvanian–Permian Cutler Formation (Colorado, U.S.A.): *Journal of Sedimentary Research*, v. 85, p. 1310–1322.
- Kleman, J., 1990, On the use of glacial striae for reconstruction of paleo-ice sheet flow patterns: *Geografiska Annaler. Series A, Physical Geography*, v. 72, p. 217.
- Kowalewski, M., Flessa, K.W., and Hallman, D.P., 1995, Ternary taphograms: Triangular diagrams applied to taphonomic analysis: *PALAIOS*, v. 10, p. 478.
- Kowalewski, M., and Labarbera, M., 2004, Actualistic taphonomy: Death, decay, and disintegration in contemporary settings: *Palaios*, v. 19, p. 423–427.

- Krinsley, D.H., and Donahue, J., 1968, Environmental interpretation of sand grain surface textures by electron microscopy: Geological Society of America Bulletin, v. 79, p. 743.
- Krinsley, D.H., Doornkamp, J.C., 1973, Atlas of quartz sand surface textures: London, U.K., Cambridge University Press, 91 p.
- Krinsley, D.H., and Smith, D.B., 1968, A selective study of grains from the Permian Yellow Sands of north-east England: Proceedings of the Geologist's Association, v. 92, p. 189-196.
- Krinsley, D.H., and Takahashi, T., 1962, Applications of electron microscopy to geology: New York Academy of Science, Transactions, v. 25, p. 3-22.
- Leeder, M.R., 1993, Tectonic controls upon drainage basin development, river channel migration and alluvial architecture: implication for hydrocarbon reservoir development and characterization, *in* North, C.P., and Prosser, D.J., eds., Characterization of Fluvial and Aeolian Reservoirs: Geological Society of London Special Publication 73, p. 7-22.
- Lidmar-Bergström, K., Ollier, C.D., and Sulebak, J.R., 2000, Landforms and uplift history of southern Norway: Global and Planetary Change, v. 24, p. 211–231.
- Lutro, O., and Tveten, E., 1996, Geological Map of Norway, berggrunskart Årdal M 1: 250,000. Geological Survey of Norway, Trondheim.
- Mahaney, W.C., 2002, Atlas of Sand Grain Surface Textures and Applications: Oxford, U.K., Oxford University Press, 256 p.

- Mahaney, W.C., Claridge, G., and Campbell, I., 1996, Microtextures on quartz grains tills from Antarctica: *Palaeogeography, Palaeoclimatology, Palaeoecology*, v. 121, p. 89-103.
- Mahaney, W.C., Dirszowsky, R.W., Milner, M.W., Menzies, J., Stewart, A., Kalm, V., and Bezada, M., 2004, Quartz microtextures and microstructures owing to deformation of glaciolacustrine sediments in the northern Venezuelan Andes: *Journal of Quaternary Science*, v. 19, p. 23–33.
- Mahaney, W.C., and Kalm, V., 1995, Scanning electron microscopy of Pleistocene tills in Estonia: *Boreas*, v. 24, p. 13–29.
- Mahaney, W.C., and Kalm, V., 2000, Comparative scanning electron microscopy study of oriented till blocks, glacial grains and Devonian sands in Estonia and Latvia: *Boreas*, v. 29, p. 35–51.
- Mahaney, W.C., Stewart, A., and Kalm, V., 2001, Quantification of SEM microtextures useful in sedimentary environmental discrimination: *Boreas*, v. 30, p. 165–171.
- Mahaney, W.C., Vortisch, W., and Julig, P., 1988, Relative differences between glacially crushed quartz transported by mountain and continental ice—some examples from North America and East Africa: *American Journal of Science*, v. 288, p. 810–826.
- Margolis, S.V., and Krinsley, D.H., 1971, Submicroscopic frosting on eolian and subaqueous quartz sand grains: *Geological Society of America Bulletin*, v. 82, p. 3395.
- Marshall, J.R., Bull, P.A., and Morgan, R.M., 2012, Energy regimes for aeolian sand grain surface textures: *Sedimentary Geology*, v. 253-254, p. 17–24.

- Masson, D.G., and Scanlon, K.M., 1991, The neotectonic setting of Puerto Rico: Geological Society of America Bulletin, v. 103, p. 144–154.
- Miall, A.D., 1996, The Geology of Fluvial Deposits; Sedimentary Facies, Basin Analysis and Petroleum Geology: Berlin, Springer, 582 p.
- Milliman, J.D., and Syvitski, J.P., 1992, Geomorphic/tectonic control of sediment discharge to the ocean: The importance of small mountainous rivers: The Journal of Geology, v. 100, p. 525–544.
- Milnes, A.G., Wennberg, O.P., Skår, Ø., and Koestler, A.G., 1997, Contraction, extension, and timing in the South Norwegian Caledonides: The Sognefjord transect, in Burg, J.-P., and Ford, M., eds., Orogeny through Time: Geological Society, London, Special Publications, p. 123–148.
- Nesbitt, H.W., Fedo, C.M., and Young, G.M., 1997, Quartz and feldspar stability, steady and non-steady-state weathering, and petrogenesis of siliciclastic sands and muds: The Journal of Geology, v. 105, p. 173–192.
- Nesbitt, H.W., Young, G.M., McLennan, S.M., and Keays, R.R., 1996, Effects of chemical weathering and sorting on the petrogenesis of siliciclastic sediments, with implications for provenance studies: The Journal of Geology, p. 525–542.
- Oliva, P., Viers, J., and Dupré, B., 2003, Chemical weathering in granitic environments: Chemical Geology, v. 202, p. 225–256.
- Østrem, G., and Haakensen, N., 1993, Glaciers of Europe—glaciers of Norway, in: Williams, R.S., and Ferrigno, J.G., (eds) Satellite image atlas of glaciers of the world: U.S. Geological Survey, Professional Paper 1386-E-3, p. E63–E109.

- Pestle, W.J., Simonetti, A., and Curet, L.A., 2013, $^{87}\text{Sr}/^{86}\text{Sr}$ variability in Puerto Rico: Geological complexity and the study of paleomobility: *Journal of Archaeological Science*, v. 40, p. 2561–2569.
- Petford, N., and Atherton, M., 1996, Na-rich partial melts from newly underplated basaltic crust: The Cordillera Blanca Batholith, Peru: *Journal of Petrology*, v. 37, p. 1491–1521.
- Pope, G.A., Dorn, R.I., and Dixon, J.C., 1995, A new conceptual model for understanding geographical variations in weathering: *Annals of the Association of American Geographers*, v. 85, p. 38–64.
- Porter, J.J., 1962, Electron microscopy of sand surface texture: *Journal of Sedimentary Petrology*, v. 32, p. 124–135.
- Pye, K., 1983, Formation of quartz silt during humid tropical weathering of dune sands: *Sedimentary Geology*, v. 34, p. 267-282.
- Pye, K., and Mazzullo, J., 1994, Effects of tropical weathering on quartz grain shape: An example from northeastern Australia: *Journal of Sedimentary Research*, v. 64, p. 500-507.
- Rea, D.K., and Janecek, T.R., 1981, Late Cretaceous history of eolian deposition in the mid-Pacific mountains, central North Pacific Ocean: *Palaeogeography, Palaeoclimatology, Palaeoecology*, v. 36, p. 55-67.
- Remeika, P., and Lindsay, L., 1992, *Geology of Anza-Borrego: Edge of Creation*: San Diego, CA, Sunbelt Publications, 207 p.

- Riebe, C.S., Kirchner, J.W., and Finkel, R.C., 2004, Erosional and climatic effects on long-term chemical weathering rates in granitic landscapes spanning diverse climate regimes: *Earth and Planetary Science Letters*, v. 224, p. 547–562.
- Rogers, C.L., Cram, C.M., Pease Jr., M.H., and Tischler, M.S., 1979, Geologic map of the Yabucoa and Punta Tuna quadrangles, Puerto Rico: IMAP Report 1086.
- Rose, K.C., and Hart, J.K., 2008, Subglacial comminution in the deforming bed: Inferences from SEM analysis: *Sedimentary Geology*, v. 203, p. 87–97.
- Rudnick, R., and Gao, S., 2003, Composition of the continental crust, *in* Rudnick, R.L., ed., *Treatise on Geochemistry*: Amsterdam, Elsevier, v. 3, p. 1–64.
- Schellekens, J.H., 1998, Geochemical evolution and tectonic history of Puerto Rico, *in* Lidiak, E.G., and Larue, D.K., eds., *Tectonics and geochemistry of the northeastern Caribbean*: Geological Society of America Special Paper 322, p. 35–66.
- Schwamborn, G., Schirrmeister, L., Frütsch, F., and Diekmann, B., 2012, Quartz weathering in freeze-thaw cycles: experiment and application to the El'gygytgyn Crater Lake record for tracing Siberian permafrost history: *Geografiska Annaler: Series A, Physical Geography*, v. 94, p. 481–499.
- Skår, Ø., and Pedersen, R.B., 2003, Relations between granitoid magmatism and migmatization: U–Pb geochronological evidence from the Western Gneiss Complex, Norway: *Journal of the Geological Society*, v. 160, p. 935–946.
- Strand, K., and Immonen, N., 2010, Dynamics of the Barents-Kara ice sheet as revealed by quartz sand grain microtextures of the late Pleistocene Arctic Ocean sediments: *Quaternary Science Reviews*, v. 29, p. 3583–3589.

- Suarez, W., Chevallier, P., Pouyaud, B., and Lopez, P., 2008, Modelling the water balance in the glacierized Parón Lake basin (White Cordillera, Peru) / Modélisation du bilan hydrique du bassin versant englacé du Lac Parón (Cordillère Blanche, Pérou): *Hydrological Sciences Journal*, v. 53, p. 266–277.
- Suttner, L.J., Basu, A., and Mack, G.H., 1981, Climate and the origin of quartz arenites: *Journal of Sedimentary Petrology*, v. 51, p. 1235-1246.
- Suzuki, K., Fujiwara, H., and Ohta, T., 2015, The evaluation of macroscopic and microscopic textures of sand grains using elliptic Fourier and principal component analysis: Implications for the discrimination of sedimentary environments: *Sedimentology*, v. 62, p. 1–14.
- Sweet, D.E., and Soreghan, G.S., 2010, Application of quartz sand microtextural analysis to infer cold-climate weathering in the equatorial Fountain Formation (Pennsylvanian–Permian, Colorado): *Journal of Sedimentary Research*, v. 80, p. 666-677.
- Thomas, M.C., Wiltshire, R.J., and Williams, A.T., 1995, The use of Fourier descriptors in the classification of particle shape: *Sedimentology*, v. 42, p. 635–645.
- Tucker, G.E., 2004, Drainage basin sensitivity to tectonic and climatic forcing: Implications of a stochastic model for the role of entrainment and erosion thresholds: *Earth Surface Processes and Landforms*, v. 29, p. 185–205.
- Tucker, G.E., and Slingerland, R., 1997, Drainage basin responses to climate change: *Water Resources Research*, v. 33, p. 2031–2047.

- Vos, K., Vandenberghe, N., and Elsen, J., 2014, Surface textural analysis of quartz grains by scanning electron microscopy (SEM): From sample preparation to environmental interpretation: *Earth-Science Reviews*, v. 128, p. 93–104.
- Wellendorf, W., and Krinsley, D., 1980, The relation between the crystallography of quartz, and upturned aeolian cleavage plates: *Sedimentology*, v. 27, p. 447–453.
- Whipple, K.X., Kirby, E., and Brocklehurst, S.H., 1999, Geomorphic limits to climate-induced increases in topographic relief: *Nature*, v. 401, p. 39–43.
- White, A.F., Blum, A.E., Schulz, M.S., Vivit, D.V., Stonestrom, D.A., Larsen, M., Murphy, S.F., and Eberl, D., 1998, Chemical weathering in a tropical watershed, Luquillo Mountains, Puerto Rico: I. long-term versus short-term weathering fluxes: *Geochimica et Cosmochimica Acta*, v. 62, p. 209–226.
- White, A.F., Blum, A.E., Bullen, T.D., Vivit, D.V., Schulz, M., and Fitzpatrick, J., 1999, The effect of temperature on experimental and natural chemical weathering rates of granitoid rocks: *Geochimica et Cosmochimica Acta*, v. 63, p. 3277–3291.
- White, A.F., and Brantley, S.L., 2003, The effect of time on the weathering of silicate minerals: Why do weathering rates differ in the laboratory and field? *Chemical Geology*, v. 202, p. 479–506.
- Williams, P.F., and Rust, B.R., 1969, The sedimentology of a braided river: *Journal of Sedimentary Petrology*, v. 39, p. 649-679.
- Woronko, B., 2016, Frost weathering versus glacial grinding in the micromorphology of quartz sand grains: Processes and geological implications: *Sedimentary Geology*, v. 335, p. 103–119.

Appendix A: Tables

Table 1. Bedrock lithologic details of the sample sites.			
Location	Lithology	Age	Average Modal Composition
Puerto Rico	Granodiorite	Cretaceous	51% plg, 20.5% qtz, 11% kspr, 11% hbl, 4.5% btt, 1.5% mag, 0.5% acc
Puerto Rico	Diorite	Cretaceous	63% plg, 25% hbl, 5% cpx, 3.5% qtz, 3% mag, 0.5% acc
Puerto Rico	Metavolcanic Rocks	Cretaceous	Plg, hbl, and act. Minor cpx, qtz, and secondary kspr.
Norway	Granite/Granodiorite	Proterozoic	–
Norway	Quartz Monzonite	Proterozoic	–
Norway	Dioritic/Granitic Gneiss	Ordovician to Devonian Metamorphism	–
California	Tonalite	Cretaceous	49% plg, 33% qtz, 10% btt, 6% kspr, 2% acc
Peru	Leucogranodiotite	Miocene	Qtz, btt, musc, plg, kspar

qtz = quartz; plg = plagioclase feldspar; hbl = hornblende; mag = magnetite; cpx = clinopyroxene; btt = biotite; musc = muscovite; kspr = potassium feldspar; aug = augite; acc = accessory minerals; Rogers et al., 1979; Lutro and Tveten, 1996; Clinkenbeard and Walawender, 1989, Petford and Atherson, 1996

Table 2. Climate, transect, and basin details of study sites.

Study Site	River Name	Climate	Transect Length (km)	Samples Analyzed	Intersample Distance	MAT (°C)	MAP (mm)	Relief (m)	Drainage Basin Area (km ²)
Puerto Rico	Guayanés	Hot/Humid	15	6	3.0	26.5	2000	483	44
Norway	Auster/Storelvi	Cold/Humid	15	7	2.5	5.5	1100	1625	160
California	Indian Gorge	Hot/Arid	7	5	1.8	22.6	150	943	23
Peru (Proximal)	Parón	Cold/Semi-arid to Arid	8.9	2	8.9	7.1-15.7	252-787	3356	85

Note: See text for sources.

Table 3. Sample sizes and size fractions used in previous quartz microtextural studies.

Study	# Grains Analyzed	Size Fraction (μm)
Armstrong-Altrin and Natalhy-Pineda (2014)	20	200 – 400
Vos et al. (2014)	10-15	100 – 2000
Immonen (2013)	30	250 – 600
Keiser et al. (2015)	20-40	250 – 1000
Costa et al. (2012)	15-20	125 – 500
Deane (2010)	>100	150 – 250
Sweet and Soreghan (2010)	10-55	300 – 3000
Chakroun et al. (2009)	10	300 – 500
Mahaney et al. (2004)	50	63 – 250
Mahaney (2002)	20	250 – 500, 500 – 2000
Mahaney and Kalm (2000)	25	63 – 2
Helland et al. (1997)	35-40	200 – 1000
Pye and Mazzulo (1994)	~100	63 – 250
Campbell and Thompson (1991)	30	125 – 2000
Mahaney et al. (1988)	20-30	63 – 250

Table 4. Quartz surface microtexture descriptions, abbreviations, and inferred formation processes.

Microtexture	Abbreviation	Description	Formation Process
Abrasion Features	af	Rubbed or worn surface	Polygenetic
Arc-Shaped Steps	as	Deep tears or breaks caused by impact Several microns deep and typically spaced > 5 μm apart	Polygenetic
Breakage Blocks	bb	Blocky void marking removal of material, typically along an edge	Polygenetic
Conchoidal Fractures	cf	Smooth curved fracture	Polygenetic
Crescentic Gouges	crg	Crescent-shaped gouges with convex and concave limbs that have depths > 5 μm	High-Stress
Curved Grooves	cg	Curved abrasion feature caused by sustained high-stress contact with another grain, < 5 μm deep	High-Stress
Deep Troughs	dt	Grooves > 10 μm deep	High-Stress
Dissolution Etching	de	Cavities from chemical dissolution; often crystallographically oriented	Chemical
Edge Rounding	er	Rounded edges on grains	Percussion
Fracture Faces	ff	Smooth and clean fractures	Polygenetic
Linear Steps	ls	Widely spaced linear features, typically > 5 μm apart	Polygenetic
Upturned Plates	up	Surfaces of impact where plates of variable size partially torn from surface, typically > 5 μm	Polygenetic
Precipitation Features	pf	Coatings of amorphous silica precipitation	Chemical
Sharp Angular Features	saf	Distinct sharp edges on grain surface	Polygenetic
Straight Grooves	sg	Linear grooves < 10 μm deep	High-Stress
Subparallel Linear Fractures	slf	Linear fractures, typically < 5 μm spacing	Polygenetic
V-Shaped Percussion Cracks	vc	V-shaped fractures or indentions with typical sizes ranging from 1 μm to 30 μm	Percussion

Compiled from results in Campbell and Thomas, 1991; Helland, 1997; Mahaney and Kalm, 2000; Mahaney, 2002; Deane, 2010; Sweet and Soreghan, 2010.

Table 5. Total number of texture counts and percent occurrence of microtextures for each location.

Statistic	pf	de	ff	slf	cf	cg	sg	dt	erg	as	ls	saf	up
<i>Norway</i>													
Sum	127	282	40	236	264	16	7	6	55	187	228	42	89
% Occurrence	0.37	0.82	0.12	0.68	0.76	0.05	0.02	0.02	0.16	0.54	0.66	0.12	0.26
<i>California</i>													
Sum	74	198	14	169	184	5	15	8	56	130	135	39	111
% Occurrence	0.30	0.79	0.06	0.68	0.74	0.02	0.06	0.03	0.22	0.52	0.54	0.16	0.44
<i>Puerto Rico</i>													
Sum	180	263	12	190	208	6	9	4	48	136	158	51	104
% Occurrence	0.61	0.89	0.04	0.64	0.70	0.02	0.03	0.01	0.16	0.46	0.53	0.17	0.35
<i>Peru</i>													
Sum	27	74	18	77	73	2	4	6	17	38	49	8	42
% Occurrence	0.27	0.74	0.18	0.77	0.73	0.02	0.04	0.06	0.17	0.38	0.49	0.08	0.42

Table 5 cont.

Statistic	vc	er	bb	af	r to sr*	sr to sa†	sa to a‡	Low Relief	Medium Relief	High Relief
<i>Norway</i>										
Sum	117	118	26	39	2	176	168	8	184	151
% Occurrence	0.34	0.34	0.08	0.11	0.01	0.51	0.49	0.02	0.53	0.44
<i>California</i>										
Sum	76	66	29	41	1	74	175	10	155	83
% Occurrence	0.30	0.26	0.12	0.16	0.00	0.30	0.70	0.04	0.62	0.33
<i>Puerto Rico</i>										
Sum	118	98	21	28	2	108	187	4	167	125
% Occurrence	0.40	0.33	0.07	0.09	0.01	0.36	0.63	0.01	0.56	0.42
<i>Peru</i>										
Sum	15	34	5	3	8	52	40	6	52	35
% Occurrence	0.15	0.34	0.05	0.03	0.08	0.52	0.40	0.06	0.52	0.35
<i>Note:</i> See Table 4 for key to abbreviations.										
* r to sr = rounded to sub-rounded										
† sr to sa = sub-rounded to sub-angular										
‡ sa to a = sub-angular to angular										

Table 6. Eigenvalues and variance for both PCA runs.

Data Set	Component	Eigenvalue	Variation (%)	Cumulative Variation (%)
All Textures	PC 1	0.040	31.31	31.31
All Textures	PC 2	0.022	17.02	48.32
All Textures	PC 3	0.018	14.11	62.44
Mechanical	PC 1	0.022	26.76	26.76
Mechanical	PC 2	0.017	20.25	47.01
Mechanical	PC 3	0.013	15.96	62.97

Table 7. Loadings of the PCA results representing all microtextures.

Microtexture	PC 1	PC 2	PC 3
pf	0.889	-0.228	0.017
de	0.077	0.235	0.394
ff	-0.132	-0.127	-0.017
slf	-0.219	0.133	0.082
cf	-0.107	-0.467	-0.128
cg	-0.029	-0.053	0.057
sg	-0.042	-0.041	-0.059
dt	-0.073	-0.022	-0.069
crg	-0.041	0.001	-0.120
as	-0.111	0.202	0.421
ls	-0.134	-0.167	0.563
saf	0.103	0.108	0.058
up	0.094	0.678	-0.374
vc	0.243	0.288	0.375
er	0.074	-0.081	0.113
bb	0.038	0.085	-0.054
vc	-0.042	-0.010	0.024

Note: See Table 4 for key to abbreviations.

Table 8. Loadings of the PCA results representing mechanical microtextures.

Microtexture	PC 1	PC 2	PC 3
ff	-0.162	0.143	0.340
slf	-0.039	0.007	0.107
cf	-0.435	-0.224	0.005
cg	-0.070	0.024	-0.063
sg	-0.051	-0.078	0.050
dt	-0.044	-0.058	0.085
crg	-0.001	-0.101	0.126
as	0.064	0.635	0.129
ls	-0.329	0.624	0.200
saf	0.140	0.094	-0.052
up	0.716	-0.034	0.503
vc	0.336	0.303	-0.707
er	-0.053	0.112	-0.053
bb	0.112	-0.010	-0.029
af	-0.034	-0.056	-0.168

Note: See Table 4 for key to abbreviations.

Appendix B: Figures

Figure 1. Locations of the four sites in this study, showing bedrock lithology, main river, tributaries, and sample collection sites. Sample collection sites are indicated by a circle with a number inset. Smaller numbers are more proximal. **A)** Puerto Rico (modified after Rogers et al. 1979). **B)** Norway (modified after Lutro and Tveten, 1996). **C)** Anza-Borrego, California (modified after Strand, 1962). **D)** Peru (modified after Giovanni et al., 2010).

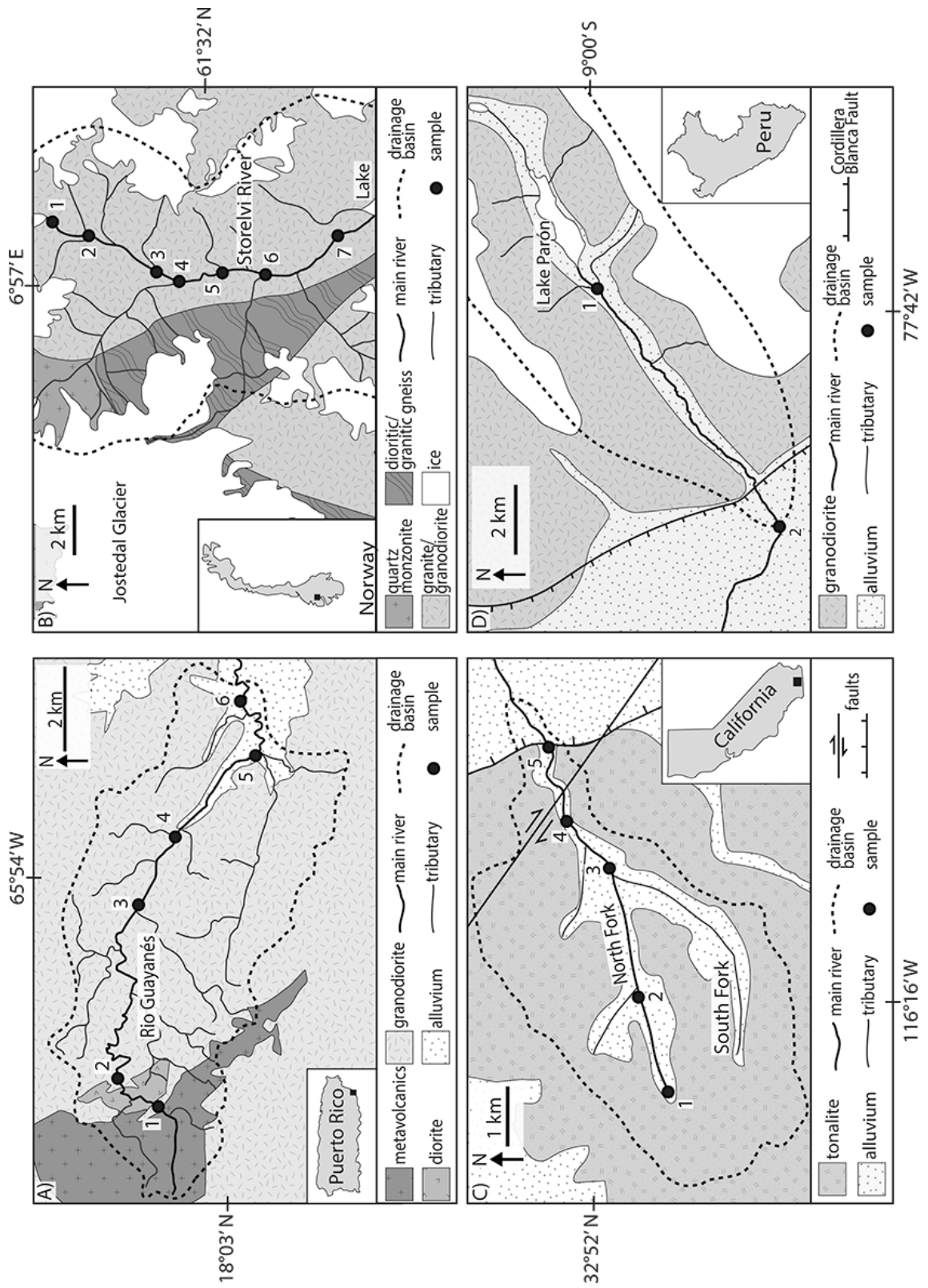


Figure 2. Photos illustrating each study location. **A)** Rio Guayanés, Puerto Rico. **B)** Storelvi River, Norway. **C)** Indian Gorge, Anza-Borrego, California. **D)** Proximal Parón drainage (lake), Peru.



Figure 3. Selected textures documented in this study. **A)** Grid layout of individual grains on a SEM stub. **B)** Grain surface displaying a v-shaped crack (vc) and triangular dissolution etching (de). **C)** Straight groove (sg) and a curved groove (cg). **D)** Grain showing arc-shaped steps (as). **E)** Deep trough (dt) on an angular grain. **F)** Grain showing heavy precipitation features (pf). **G)** Angular grain with precipitation features (pf) covering the bottom half of the grain. Linear steps (ls), dissolution etching (de), and conchoidal fractures (cf) populate the upper half. **H)** Zoomed view of triangular dissolution etching (de). Note that all dissolution etch pits have the same orientation. **I)** Grain surface showing upturned plate (up).

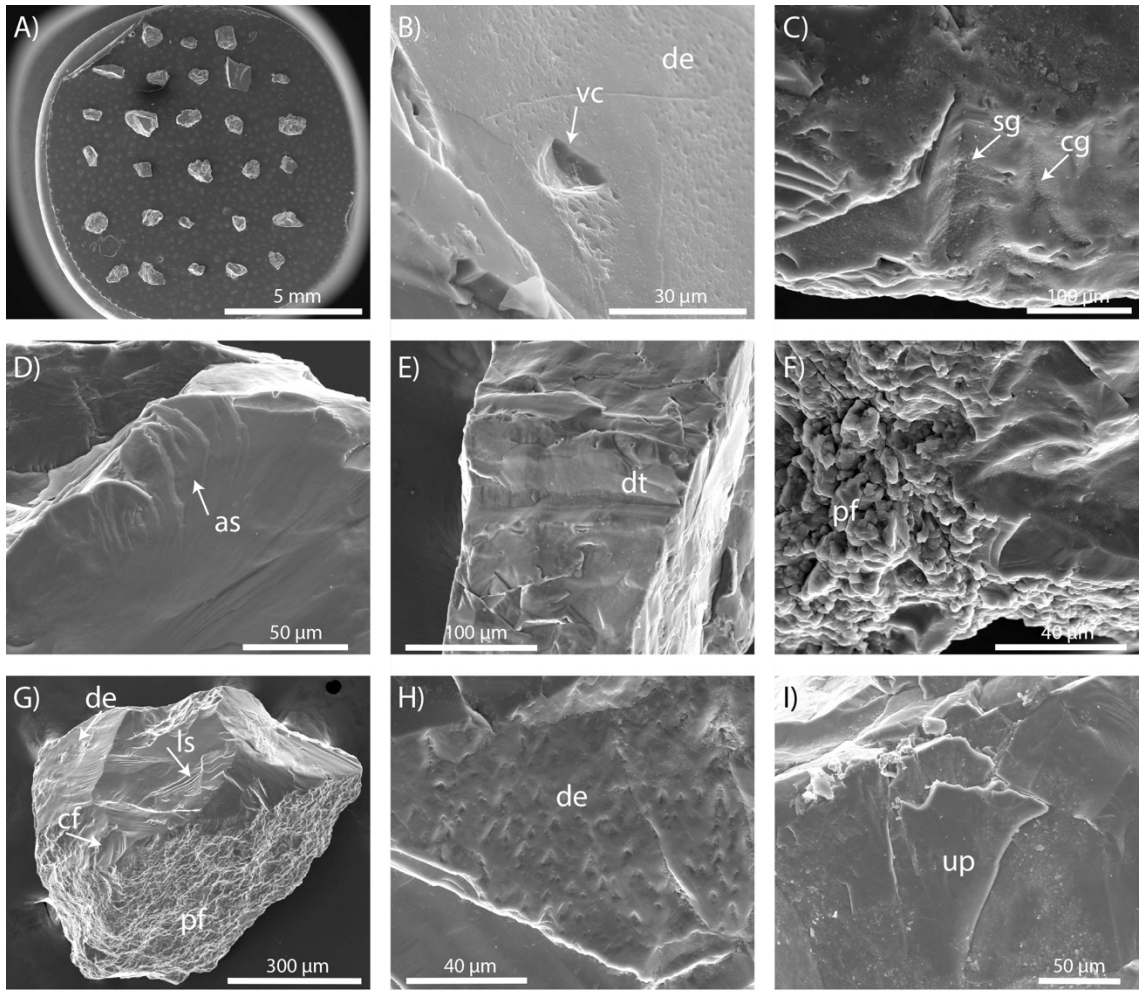


Figure 4. Selected textures documented in this study. **A)** Sub-angular grain with abrasion features (af) covering the top of the grain. **B)** Grain with multiple breakage blocks (bb). **C)** Sub-angular grain with a very clear fracture face (ff). **D)** A close up view of subparallel linear fractures (slf). **E)** Angular grain with multiple large conchoidal fractures (cf) and linear steps (ls). **F)** Grain showing the occurrence of both precipitation features (pf) and dissolution etching (de) in close proximity. **G)** Angular grain with a crescentic gauge (crg), arc-shaped steps (as), and precipitation features (pf). **H)** Sub-angular grain with multiple conchoidal fractures (cf) along a rounded edge (er), along with linear steps (ls) and dissolution etching (de). **I)** Angular grain uncommonly devoid of any chemical features displaying fresh surfaces in the form of fractures faces (ff). Also displays conchoidal fractures (cf), linear steps (fs), subparallel linear fractures (slf), and sharp angular features (saf).

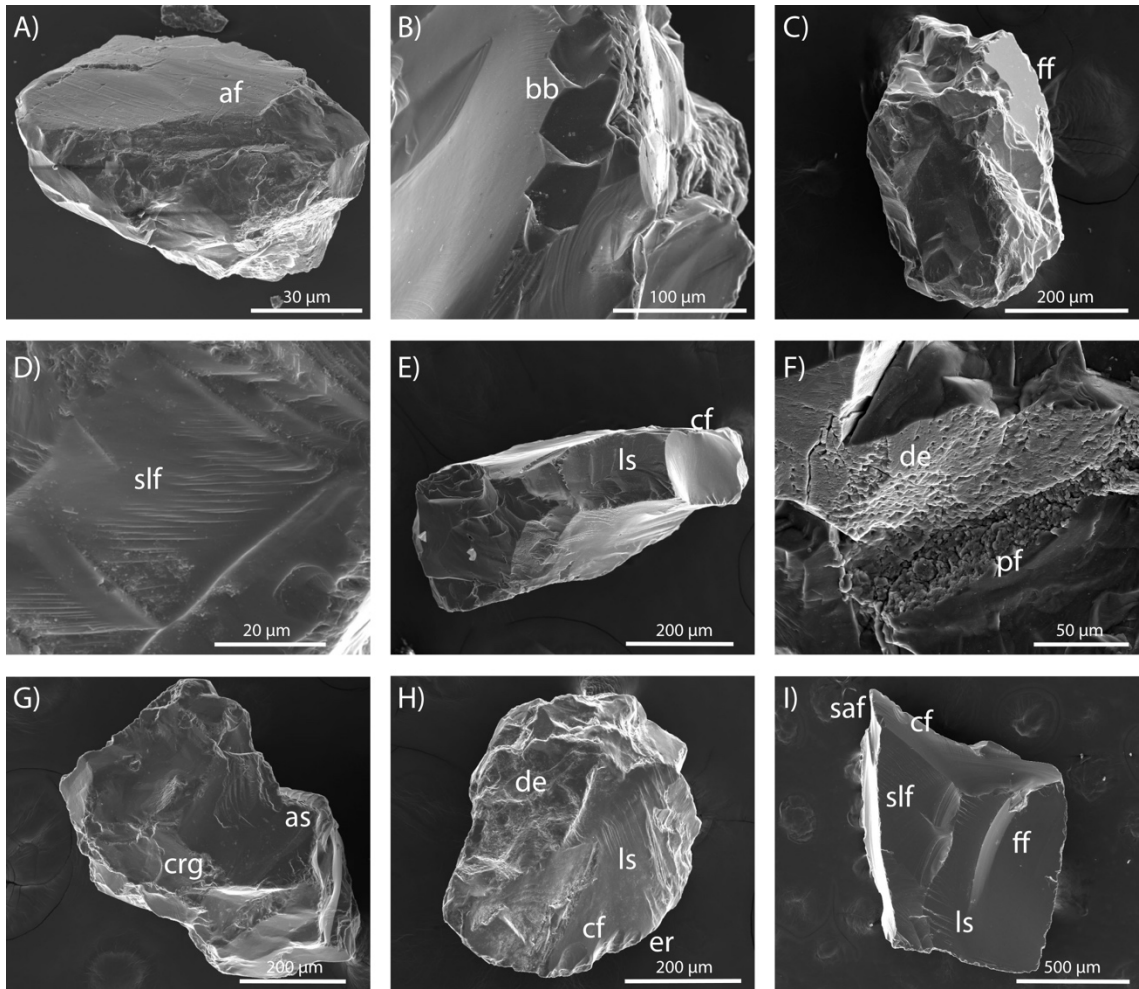
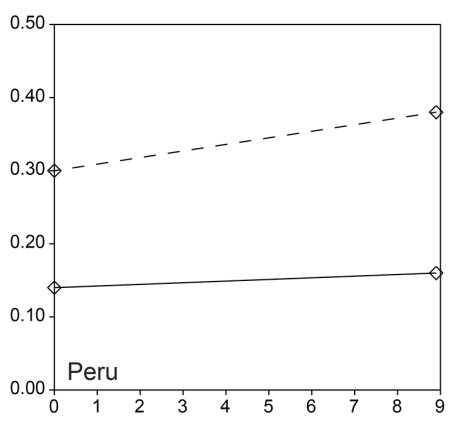
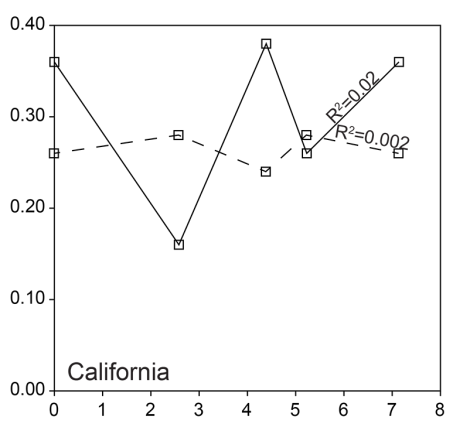
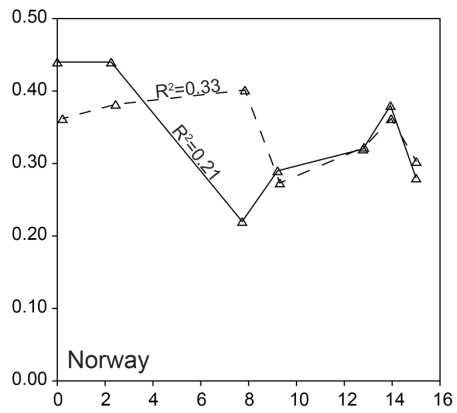
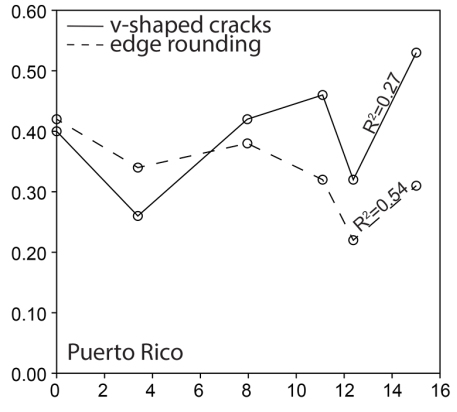


Figure 5. Occurrences of percussion-induced fractures, edge rounding (er) and v-shaped percussion cracks (vc), plotted by sampling locations, from proximal (left) to distal (right). The R^2 values of the trend lines for Puerto Rico, Norway, and California are displayed. The trend lines themselves are omitted to reduce clutter in the plots.

Occurrence of Percussion-Induced Microtextures



Distance (km)

Figure 6. Plots from PCA analysis of all textures. **A)** Scatter of variables projected onto PC1 and PC2. **B)** Scatter plot of sites plotted onto projections of PC1 and PC2. **C)** Scatter plot of variables plotted onto PC1 and PC3. **D)** Scatter plot of sample projected onto PC1 and PC3. These projected scatter plots aid segregation of data. See text for detailed explanation.

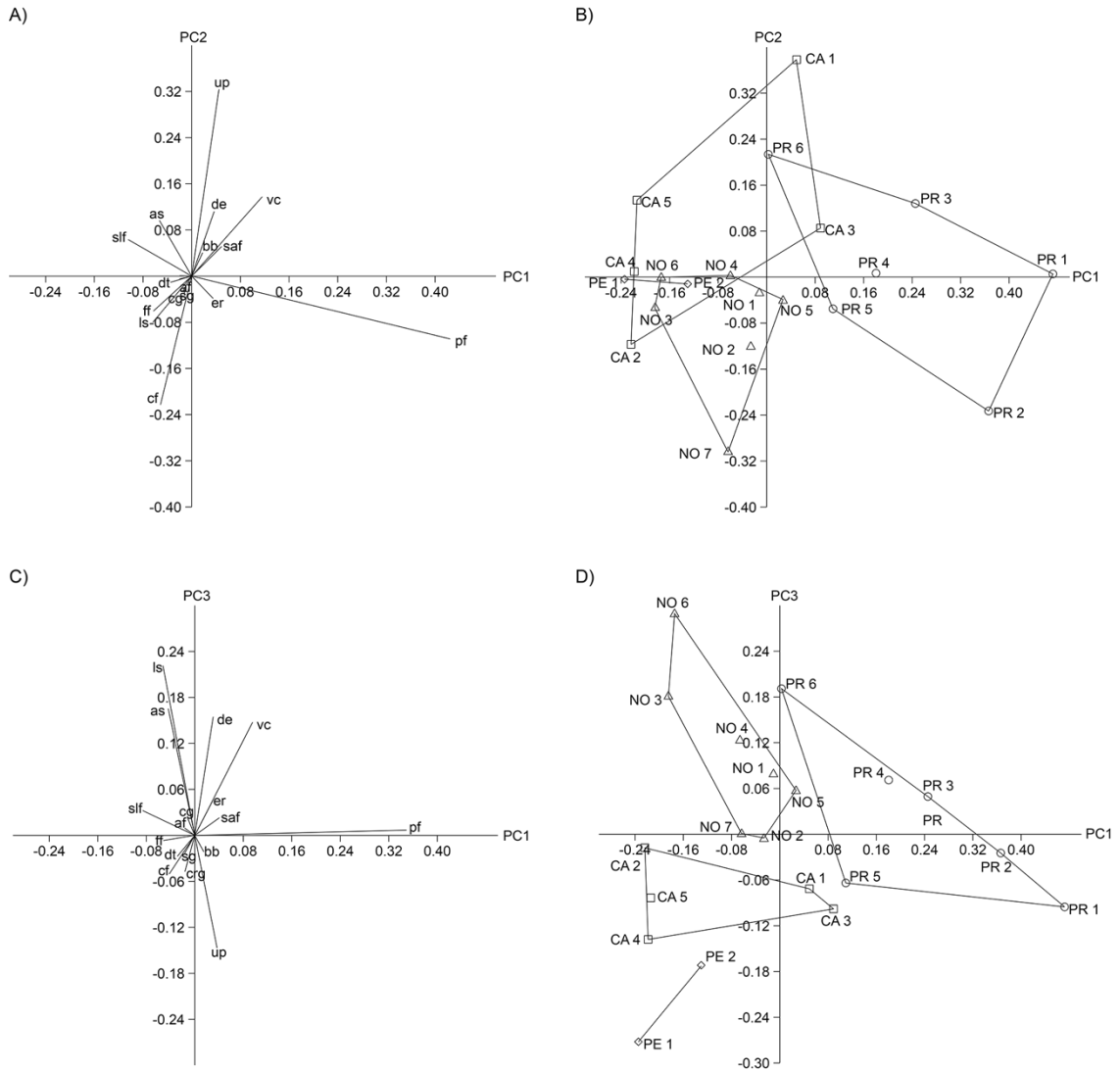


Figure 7. Plots from PCA analysis of mechanical textures only. **A)** Scatter of variables projected onto PC1 and PC2. **B)** Scatter plot of sites plotted onto projections of PC1 and PC2. **C)** Scatter plot of variables plotted onto PC1 and PC3. **D)** Scatter plot of samples projected onto PC1 and PC3. These projected scatter plots aid segregation of data. See text for detailed explanation.

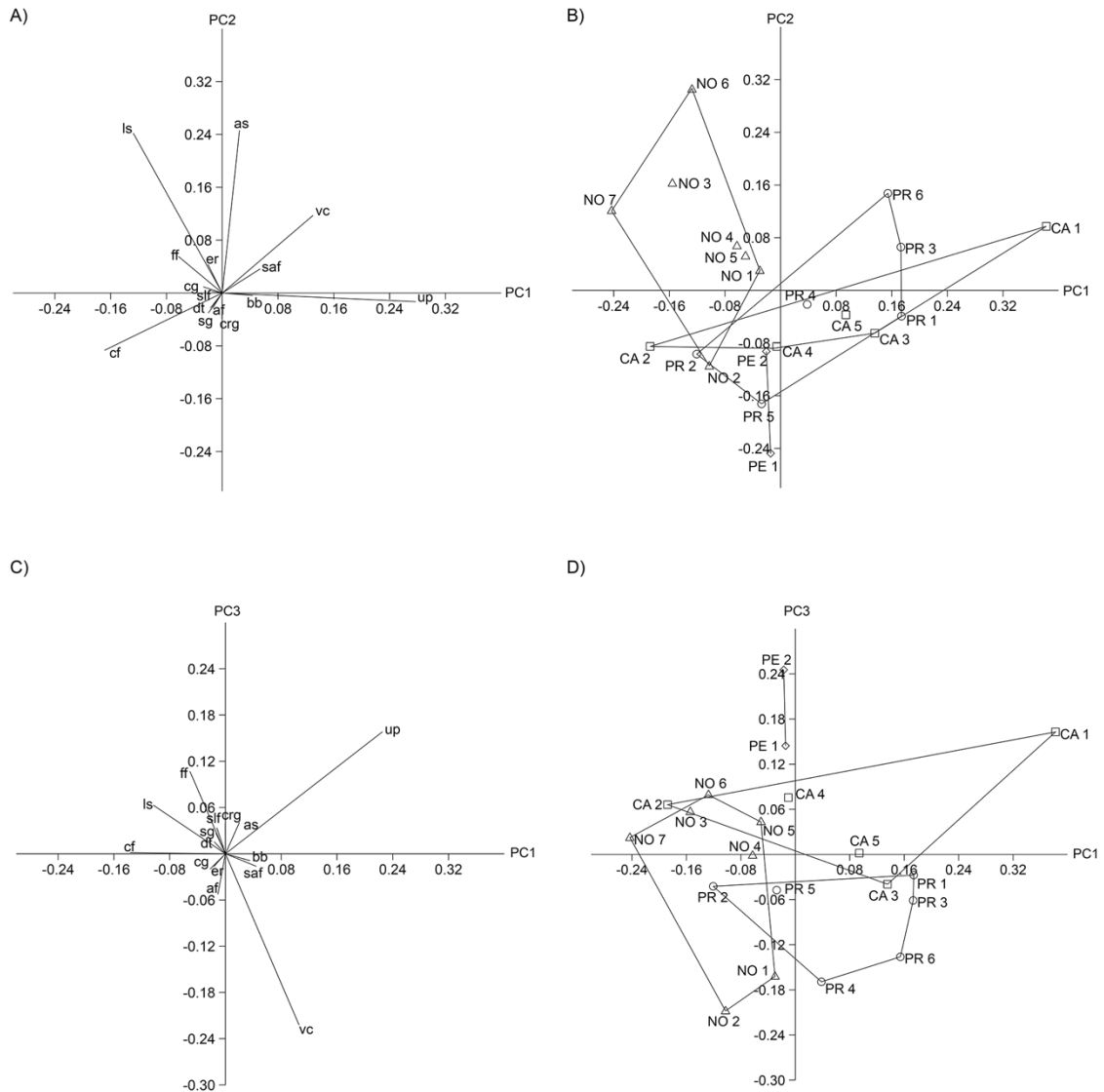


Figure 8. Abundances of v-shaped cracks (vc), precipitation features (pf), upturned plates (up), fracture faces (ff), and subparallel linear fractures (slf). The most proximal samples are illustrated with filled symbols.

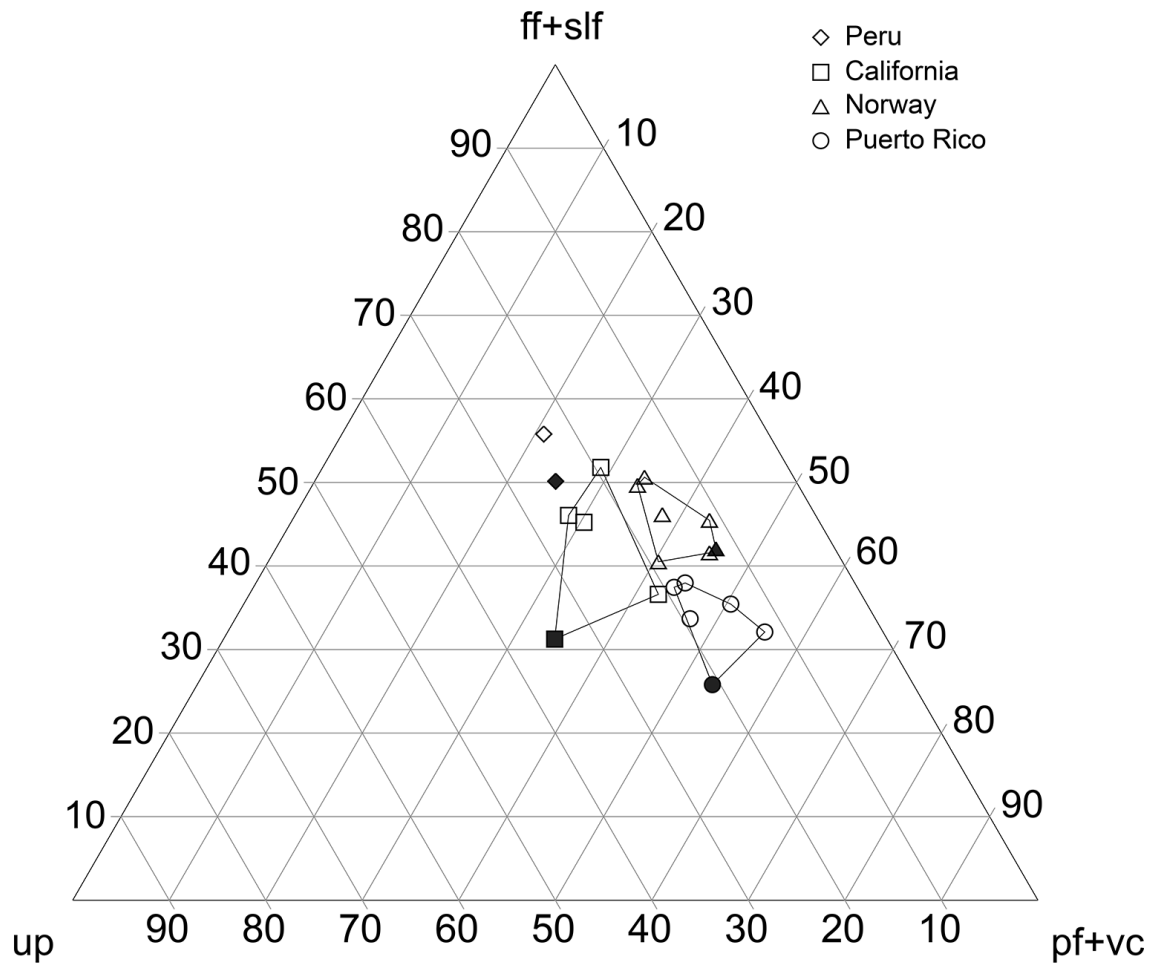
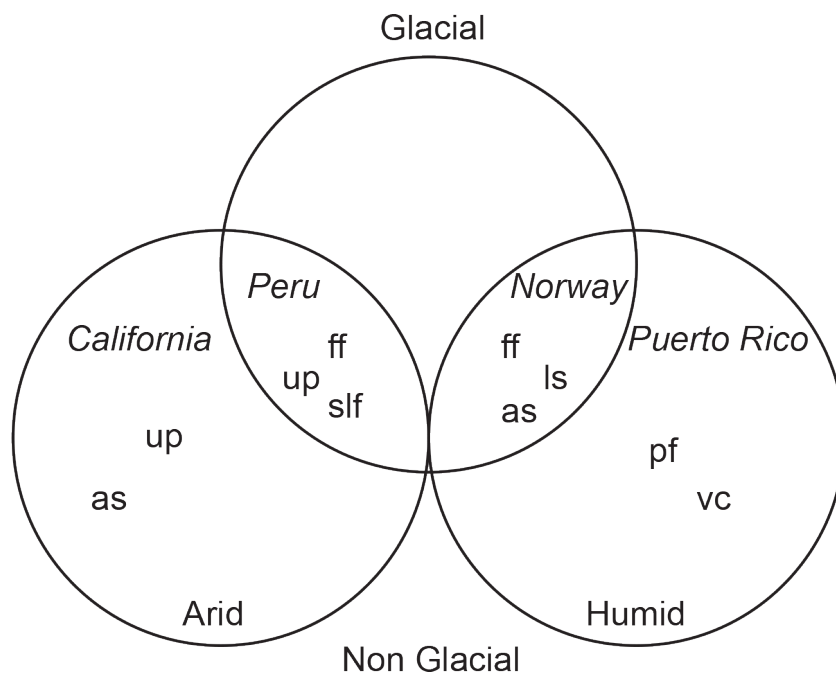


Figure 9. Venn diagram illustrating which locations and microtextures are associated with which environmental conditions. See Table 4 for key to abbreviations.



Appendix C: Microtexture Count Raw Data

Notes: The following tables contain the scores assigned to each grain of every sampling location. See Table 4 for key to microtexture abbreviations. PR = Puerto Rico, NOR = Norway, and CAL = California. There are two tables for every sampling location where the first table is for the first ~25 grains and the second table is for the second ~25 grains.

Sample #	Date	NOR 1A	# Grains	25		12		11		10		9		8		7		6		5		4		3		2		1	
				Low	Medium	High	ff	pf	de	sif	cf	cg	sg	dt	crg	as	ls	saf	up	vc	er	bb	af						
1	0	0	1	0	0	1	1	1	0	0	0	0	0	1	0	0	0	0	0	0	0	0	0	0	0	0	0	0	
2	0	1	0	0	1	0	1	0	0	1	1	0	0	1	0	0	0	0	0	0	0	0	0	0	0	0	0	0	0
3	0	1	0	0	1	0	1	1	0	1	1	0	0	1	0	0	0	0	0	0	0	0	0	0	0	0	0	0	0
4	0	0	1	0	1	0	1	1	0	0	1	1	0	0	0	0	0	0	0	0	0	0	0	0	0	0	0	0	0
5	0	0	1	0	0	1	1	1	0	0	1	1	0	0	0	0	0	0	0	0	0	0	0	0	0	0	0	0	0
6	0	1	0	0	1	0	1	1	0	0	1	1	0	0	0	0	0	0	0	0	0	0	0	0	0	0	0	0	0
7	0	1	0	0	1	0	1	1	0	0	1	1	0	0	0	0	0	0	0	0	0	0	0	0	0	0	0	0	0
8	0	1	0	0	1	0	1	1	0	0	1	1	0	0	0	0	0	0	0	0	0	0	0	0	0	0	0	0	0
9	0	0	1	0	1	0	1	0	0	1	0	0	1	0	0	0	0	0	0	0	0	0	0	0	0	0	0	0	0
10	0	1	0	0	0	1	0	1	0	0	1	1	0	0	0	0	0	0	0	0	0	0	0	0	0	0	0	0	0
11	0	1	0	0	0	1	0	1	0	0	1	1	0	0	0	0	0	0	0	0	0	0	0	0	0	0	0	0	0
12	0	1	0	0	0	1	0	1	0	0	1	1	0	0	0	0	0	0	0	0	0	0	0	0	0	0	0	0	0
13	0	1	0	0	0	1	0	1	0	0	1	1	0	0	0	0	0	0	0	0	0	0	0	0	0	0	0	0	0
14	0	0	1	0	0	1	0	1	0	0	1	1	0	0	0	0	0	0	0	0	0	0	0	0	0	0	0	0	0
15	0	0	1	0	0	1	0	1	0	0	1	1	0	0	0	0	0	0	0	0	0	0	0	0	0	0	0	0	0
16	0	0	1	0	0	1	0	1	0	0	1	1	0	0	0	0	0	0	0	0	0	0	0	0	0	0	0	0	0
17	0	1	0	0	0	1	0	1	0	0	1	1	0	0	0	0	0	0	0	0	0	0	0	0	0	0	0	0	0
18	0	1	0	0	0	1	0	1	0	0	1	1	0	0	0	0	0	0	0	0	0	0	0	0	0	0	0	0	0
19	0	0	1	0	0	1	0	1	0	0	1	1	0	0	0	0	0	0	0	0	0	0	0	0	0	0	0	0	0
20	0	1	0	0	0	1	0	1	0	0	1	1	0	0	0	0	0	0	0	0	0	0	0	0	0	0	0	0	0
21	0	1	0	0	0	1	0	1	0	0	1	1	0	0	0	0	0	0	0	0	0	0	0	0	0	0	0	0	0
22	0	1	0	0	0	1	0	1	0	0	1	1	0	0	0	0	0	0	0	0	0	0	0	0	0	0	0	0	0
23	0	0	1	0	0	1	0	1	0	0	1	1	0	0	0	0	0	0	0	0	0	0	0	0	0	0	0	0	0
24	0	0	1	0	0	1	0	1	0	0	1	1	0	0	0	0	0	0	0	0	0	0	0	0	0	0	0	0	0
25	0	1	0	0	0	1	0	1	0	0	1	1	0	0	0	0	0	0	0	0	0	0	0	0	0	0	0	0	0
Count	0	15	10	0	12	12	11	19	19	16	0	0	0	5	10	17	7	11	11	3	1	0	0	0	0	0	0	0	0
%	0	0.6	0.4	0	0.48	0.48	0.44	0.76	0.76	0.64	0	0	0	0.2	0.4	0.68	0.28	0.44	0.44	0.12	0.04	0	0	0	0	0	0	0	0

Sample Date	NOR 1B 1/6/16	# Grains	25																			
#	r to sr	sr to sa	sa to																			
			Low	Medium	High	ff	pf	de	sif	cf	cg	sg	dt	crg	as	ls	saf	up	vc	er	bb	af
1	0	1	0	1	0	0	1	1	1	1	0	0	0	0	1	0	0	0	1	0	0	0
2	0	0	1	0	0	0	0	1	0	0	0	0	0	0	1	1	0	0	0	1	0	0
3	0	0	1	0	1	0	0	1	1	1	0	0	0	0	0	1	0	0	0	0	1	0
4	0	0	1	0	1	0	0	0	1	1	0	0	0	0	1	1	1	0	0	0	0	1
5	0	0	1	0	0	0	1	1	1	1	0	0	0	0	1	0	0	0	0	0	0	0
6	0	1	0	0	1	0	0	1	1	0	0	0	0	1	0	0	1	1	1	1	0	0
7	0	1	0	0	1	0	0	1	1	0	0	0	0	0	0	0	1	1	0	0	0	0
8	0	1	0	0	1	0	0	1	1	1	0	0	0	0	1	1	0	0	1	1	0	0
9	0	1	0	0	1	0	0	1	0	0	1	0	0	0	1	1	0	0	0	1	0	0
10	0	1	0	0	0	0	1	0	1	0	0	0	0	0	1	0	0	1	0	0	0	0
11	0	1	0	0	1	0	0	1	1	0	0	0	0	1	0	0	0	0	0	1	0	0
12	0	0	1	0	0	0	0	0	1	0	0	1	0	0	0	1	0	0	1	0	0	1
13	0	1	0	0	0	0	0	1	1	1	0	0	0	0	0	0	0	0	1	1	0	0
14	0	0	1	0	0	0	0	1	1	1	0	0	0	0	0	1	0	0	0	0	1	0
15	0	1	0	0	1	0	0	1	0	1	0	0	0	0	0	0	0	0	1	0	1	0
16	0	1	0	0	1	0	0	1	1	1	0	0	0	0	1	1	0	0	1	0	1	1
17	0	0	1	1	0	0	0	1	0	1	0	0	0	0	1	0	0	0	0	0	0	1
18	0	0	1	1	0	0	1	0	0	0	0	0	0	0	1	0	0	0	1	0	0	1
19	0	0	1	0	1	0	0	1	0	1	0	0	0	0	0	0	0	0	0	0	0	0
20	0	1	0	0	1	0	0	1	1	1	0	0	0	0	0	0	0	0	0	0	0	0
21	0	1	0	0	1	0	0	1	0	1	0	0	0	1	1	0	0	0	0	0	0	0
22	0	0	1	0	0	0	0	1	1	1	0	0	0	0	0	1	0	0	0	0	0	0
23	0	0	1	0	1	0	0	0	1	1	1	0	0	1	1	1	0	0	0	0	0	0
24	0	1	0	0	1	0	0	1	0	1	0	0	0	0	0	1	0	1	1	0	0	0
25	0	1	0	0	1	0	0	1	1	1	0	0	0	0	1	0	0	0	1	1	1	0
Count	0	13	12	1	19	4	1	8	17	16	2	1	0	4	12	13	2	4	11	7	4	6
%	0	0.52	0.48	0.04	0.76	0.16	0.04	0.32	0.68	0.64	0.08	0.04	0	0.16	0.48	0.52	0.08	0.16	0.44	0.28	0.16	0.24

Sample #	NOR 2A Date	# Grains	25			Low	Medium	High	ff	pf	de	sif	cf	cg	sg	dt	crg	as	ls	saf	up	vc	er	bb	af
			r to sr	sr to sa	sa to																				
1	0	1	0	0	0	0	1	0	1	0	1	1	0	0	0	0	1	0	0	1	0	1	0	0	
2	0	1	0	0	0	0	1	0	1	1	0	1	0	0	0	0	1	0	0	1	0	0	0	0	
3	0	1	0	0	0	1	0	0	0	1	0	0	0	0	0	0	1	0	0	0	0	0	0	0	
4	0	1	0	0	0	0	1	0	0	1	1	1	0	0	0	0	0	0	1	0	0	0	0	1	
5	0	1	0	0	0	1	0	0	0	1	1	1	0	0	0	0	1	0	0	0	1	0	0	1	
6	0	1	0	0	0	1	0	0	0	1	1	1	1	0	0	0	1	0	0	0	1	1	0	0	
7	0	0	1	0	0	0	1	0	0	1	1	1	0	0	0	0	1	0	0	0	0	1	0	0	
8	0	1	0	0	0	0	1	0	0	1	1	1	0	0	0	1	1	0	0	0	0	0	0	0	
9	0	1	0	0	0	0	1	0	0	1	1	1	0	0	0	1	0	0	1	1	1	1	0	0	
10	0	1	0	0	0	0	1	0	1	0	1	1	0	0	0	0	0	1	0	0	0	1	0	1	
11	0	0	1	0	0	0	1	0	1	0	1	1	0	0	0	0	0	0	1	0	0	0	0	0	
12	0	1	0	0	0	0	1	0	0	1	1	1	0	0	0	0	0	1	0	0	0	0	0	1	
13	0	1	0	0	0	0	1	0	0	1	1	1	0	0	0	0	0	1	1	1	1	0	0	0	
14	0	1	0	0	0	1	0	0	0	1	0	1	0	0	0	1	0	1	0	0	1	1	0	0	
15	0	1	0	0	0	0	1	0	0	1	1	1	0	0	0	0	1	0	0	0	1	1	0	0	
16	0	1	0	0	0	1	0	0	0	1	1	1	0	0	0	0	0	0	0	1	1	1	0	0	
17	0	1	0	0	0	0	1	0	1	1	0	1	0	0	0	0	0	1	0	0	0	0	1	0	
18	0	1	0	0	0	0	1	0	1	1	1	1	0	0	0	0	1	0	0	0	0	0	0	0	
19	0	1	0	0	0	0	1	0	1	0	1	1	0	0	0	0	0	0	0	0	0	1	0	0	
20	0	0	1	0	0	1	0	0	1	0	1	1	0	0	0	1	1	1	0	0	1	0	0	0	
21	0	0	1	0	0	0	1	0	0	1	1	1	0	0	0	0	1	1	0	0	1	1	0	0	
22	0	1	0	0	0	0	1	0	0	1	1	1	0	1	0	0	0	0	0	0	0	0	0	0	
23	0	1	0	0	0	0	1	0	1	1	1	1	0	0	0	1	1	1	0	1	0	1	0	0	
24	0	1	0	0	0	0	1	1	1	1	0	1	0	0	0	0	0	0	0	0	0	1	0	0	
25	0	1	0	0	0	1	0	0	1	1	1	1	0	0	0	0	0	1	1	0	0	1	0	0	
Count	0	12	13	0	7	18	11	20	24	2	0.08	0.04	0	0	0	0.16	0.48	0.4	0.12	0.32	8	10	12	2	4
%	0	0.48	0.52	0	0.28	0.72	0.44	0.8	0.96	0.08	0.04	0	0	0	0	0.16	0.48	0.4	0.12	0.32	0.4	0.48	0.08	0.16	0.16

Sample Date	NOR 2B 10/8/15	# Grains	23																				
#	r to sr	sr to sa	sa to	Low	Medium	High	ff	pf	de	sif	cf	cg	sg	dt	crig	as	ls	saf	up	vc	er	bb	af
1	0	0	1	0	0	1	0	0	1	1	1	0	0	0	1	0	0	0	1	0	0	0	0
2	0	0	1	0	0	1	0	0	1	1	1	0	0	0	0	0	1	0	0	0	0	0	0
3	0	1	0	0	0	0	0	0	1	1	1	0	0	0	0	0	1	0	0	0	0	1	0
4	0	0	1	0	0	1	0	0	0	0	1	1	0	0	0	0	1	1	0	1	0	0	0
5	0	0	1	0	0	1	0	0	0	0	1	0	0	0	0	0	1	1	0	1	0	0	0
6	0	0	1	0	0	1	0	1	1	0	0	0	0	0	0	0	0	1	0	1	0	0	0
7	0	0	1	0	0	1	0	0	1	1	1	0	0	0	0	0	0	0	1	0	0	0	0
8	0	0	1	0	1	0	0	1	1	1	1	0	0	0	0	1	0	0	0	1	1	0	0
9	0	0	1	0	1	0	1	0	1	0	1	0	0	0	0	1	1	0	0	1	0	0	1
10	0	1	0	0	0	1	0	0	1	1	1	0	0	1	0	0	1	0	0	0	0	0	0
11	0	1	0	0	0	1	0	1	1	0	1	0	0	0	0	1	0	0	0	1	0	0	0
12	0	1	0	0	0	1	0	1	1	1	1	0	0	0	0	0	1	0	0	0	1	0	0
13	0	0	1	0	0	1	0	0	1	0	1	0	0	0	0	0	0	0	0	1	0	0	0
14	0	0	1	0	0	1	0	1	0	1	1	0	0	0	0	0	1	1	0	0	0	0	0
15	0	1	0	0	1	0	0	1	1	0	0	0	0	0	0	1	1	0	0	1	0	0	0
16	0	0	1	0	0	1	0	0	1	0	1	0	0	0	0	0	1	1	0	1	0	0	0
17	0	0	1	0	0	1	0	0	1	1	1	0	0	0	0	1	1	0	0	1	0	0	1
18	0	0	1	0	0	1	0	0	1	1	1	1	0	0	0	0	0	0	0	1	1	0	0
19	0	1	0	0	1	0	0	0	1	1	1	0	0	0	0	0	1	0	1	1	1	0	0
20	0	1	0	0	1	0	0	0	1	1	1	0	0	0	0	1	0	0	0	0	0	0	1
21	0	0	1	0	0	1	0	1	1	1	1	0	0	0	0	0	0	0	0	0	0	0	0
22	0	0	1	0	1	0	0	0	1	0	1	0	0	0	0	1	0	0	0	0	0	0	0
23	0	0	1	0	0	1	0	0	1	0	1	0	0	0	0	1	0	0	0	1	0	0	1
24																							
25																							
Count	0	6	17	0	8	15	2	6	21	12	21	3	0	1	1	9	11	4	3	11	6	1	4
%	0	0.26087	0.73913	0	0.34783	0.65217	0.087	0.26087	0.91304	0.52174	0.91304	0.13043	0	0.04348	0.04348	0.3913	0.47826	0.17391	0.13043	0.47826	0.26087	0.04348	0.17391

Sample Date	NOR AB 1/19/16	#Grains	23	sa to	Low	Medium	High	ff	pf	de	sif	cf	cg	sg	dt	crf	as	ls	saf	up	vc	er	bb	af
1	0	1	0	0	0	1	0	1	0	1	0	1	0	0	0	1	0	1	0	0	0	1	0	0
2	0	0	1	0	0	0	1	0	0	0	1	1	0	0	0	0	0	1	0	1	0	1	0	0
3	0	1	0	0	0	0	1	0	0	1	1	1	0	0	0	0	1	0	0	1	1	0	0	0
4	0	1	0	0	0	0	1	0	0	1	1	1	0	0	0	1	1	0	0	0	1	0	0	0
5	0	1	0	0	0	1	0	0	1	1	1	0	0	0	0	0	0	0	0	0	0	0	1	0
6	0	1	0	0	0	0	1	0	0	1	1	1	0	0	0	0	1	1	0	0	0	1	0	0
7	0	1	0	0	0	0	1	0	1	1	1	1	0	0	0	0	1	1	0	0	0	0	0	0
8	0	1	0	0	0	0	1	1	1	1	1	1	0	0	0	0	1	1	0	0	0	1	0	1
9	0	1	0	0	0	0	1	0	1	1	0	1	0	0	0	0	1	1	0	1	0	0	0	0
10	0	0	1	0	0	1	0	0	1	0	1	0	1	0	0	1	1	1	0	1	0	0	0	1
11	0	1	0	0	0	1	0	0	0	1	0	0	0	0	0	0	1	0	0	0	0	0	0	0
12	0	0	1	0	0	1	0	0	0	1	1	0	0	0	0	0	0	0	0	0	0	0	0	0
13	0	1	0	0	0	1	0	0	1	1	1	0	0	0	0	0	1	0	0	0	0	0	0	0
14	0	1	0	0	0	1	0	0	0	1	1	1	0	0	0	0	1	1	0	0	0	0	0	0
15	0	0	1	0	0	1	0	0	0	1	1	1	0	0	0	0	1	1	0	0	1	0	0	0
16	0	0	1	0	0	1	0	0	1	1	1	0	0	0	0	0	1	0	1	0	0	0	0	1
17	0	1	0	0	0	1	0	0	1	1	0	0	0	0	0	0	1	1	0	0	1	0	0	0
18	0	0	1	0	0	0	0	0	1	1	1	1	0	0	0	0	0	0	0	0	0	0	0	0
19	0	0	1	0	0	1	0	0	0	0	1	0	0	0	0	0	0	1	0	0	0	0	0	1
20	0	1	0	0	0	1	0	0	0	1	1	1	0	0	0	0	0	0	0	0	0	0	0	0
21	0	1	0	0	0	1	0	1	0	1	1	1	0	0	0	0	1	1	0	0	0	0	0	0
22	0	1	0	0	0	1	0	0	0	1	1	1	0	0	0	0	1	0	0	1	1	1	0	0
23	0	1	0	0	0	1	0	0	0	1	1	0	0	0	0	0	1	1	0	0	0	0	0	0
24																								
25																								
Count	0	16	7	0	0	15	8	3	9	20	19	13	1	0	0	3	16	13	1	5	5	5	1	4
%	0	0.69565	0.30435	0	0	0.65217	0.34783	0.1304	0.3913	0.86957	0.82609	0.56522	0.04348	0	0	0.13043	0.69565	0.56522	0.04348	0.21739	0.21739	0.21739	0.04348	0.17391

Sample Date	NOR-58 1/5/16	#Grains	25																								
#	r to sr	sr to sa	sa to	Low	Medium	High	ff	pf	de	slf	cf	cg	sg	dt	crg	as	ls	saf	up	vc	er	bb	af				
1	0	1	0	0	1	0	0	0	1	1	0	0	0	0	0	1	0	0	0	1	1	0	0				
2	0	1	0	0	1	0	1	1	0	1	1	0	0	0	1	0	1	1	0	0	0	1	0				
3	0	0	1	0	1	0	0	0	1	1	1	0	0	0	0	1	0	0	0	0	0	0	0				
4	0	0	1	0	1	0	1	0	1	1	1	0	0	0	0	1	1	1	1	1	0	0	0				
5	0	0	1	0	1	0	0	0	1	1	0	0	0	0	0	1	1	0	0	1	0	0	0				
6	0	0	1	0	0	1	0	1	1	0	0	0	0	0	0	1	0	1	0	0	0	0	0				
7	0	1	0	0	1	0	0	0	1	1	1	0	0	0	0	1	0	0	0	0	0	0	0				
8	0	1	0	0	1	0	0	0	1	1	1	0	0	0	0	0	1	0	1	1	1	0	0				
9	0	0	1	0	1	0	0	0	1	1	1	0	0	0	0	1	1	0	0	0	0	0	0				
10	0	0	1	0	1	0	0	0	1	0	1	0	0	0	0	1	1	0	0	0	0	0	0				
11	0	0	1	1	0	0	0	0	1	0	1	0	0	0	1	0	1	0	0	0	0	0	0				
12	0	1	0	0	1	0	0	1	1	0	1	0	0	0	0	1	1	0	0	1	1	0	0				
13	0	0	1	0	1	0	0	0	1	1	1	0	0	0	0	0	0	0	1	0	0	1	1				
14	0	0	1	0	1	0	0	0	1	1	0	0	0	0	1	0	1	0	0	0	0	0	0				
15	0	0	1	0	1	0	0	0	1	1	1	0	0	0	0	0	1	0	0	1	1	0	1				
16	0	0	1	0	1	0	0	0	1	0	1	0	0	0	0	1	1	0	1	0	0	0	0				
17	0	0	1	0	1	0	0	0	1	1	1	0	0	0	1	0	1	1	0	1	0	0	0				
18	0	1	0	0	1	0	0	0	1	1	1	0	0	0	0	0	0	0	1	0	0	0	0				
19	0	1	0	0	0	0	0	0	1	1	1	0	0	0	0	0	1	0	0	0	1	0	0				
20	0	0	1	0	1	0	0	0	1	0	0	0	0	0	0	1	1	0	1	1	0	0	0				
21	0	1	0	0	1	0	0	1	1	1	1	0	0	0	0	1	0	0	0	1	1	0	0				
22	0	0	1	1	0	0	0	1	1	1	1	0	0	0	0	1	1	0	1	0	0	0	0				
23	0	1	0	0	1	0	0	0	1	1	1	0	0	0	0	0	0	1	0	1	0	1	0				
24	0	0	1	1	0	0	0	0	0	1	0	0	0	0	0	1	1	0	1	0	0	0	0				
25	0	1	0	0	1	0	0	0	1	1	1	0	0	0	0	1	1	0	0	0	0	0	1				
Count	0	10	15	3	20	2	2	9	23	18	20	0	0	0	4	15	18	3	9	8	8	1	3				
%	0	0.4	0.6	0.12	0.8	0.08	0.08	0.36	0.92	0.72	0.8	0	0	0	0.16	0.6	0.72	0.12	0.36	0.32	0.32	0.04	0.12				

Sample Date	NOR 6A 1/19/16	#Grains	25	sa to	sr to sr	Low	Medium	High	ff	pf	de	sif	cf	cg	sg	dt	crg	as	ls	saf	up	vc	er	bb	af
1	0	1	0	0	1	0	1	0	0	0	1	1	1	0	0	0	0	1	0	0	0	0	1	0	0
2	0	1	0	0	1	0	1	0	0	1	1	1	1	0	0	0	0	1	1	1	0	0	1	0	0
3	0	1	0	0	1	0	1	0	0	1	1	1	1	0	0	0	0	0	1	1	0	1	0	0	0
4	0	1	0	0	1	0	1	0	0	1	1	1	1	0	0	0	0	1	1	1	0	0	1	0	0
5	0	0	1	0	0	0	1	1	0	1	1	1	1	0	0	0	0	1	1	1	0	0	1	0	0
6	0	0	1	0	0	0	1	1	0	1	1	1	1	0	0	0	1	1	1	1	0	0	0	0	1
7	0	0	1	0	0	0	1	1	0	1	1	1	1	0	0	0	0	1	1	1	1	1	0	0	0
8	0	1	0	1	0	0	1	0	0	0	1	1	1	0	0	0	1	0	1	0	0	1	0	0	0
9	0	1	0	0	0	0	1	1	0	0	1	1	1	0	0	0	0	1	1	1	0	0	0	0	0
10	0	1	0	0	0	0	1	1	0	0	1	1	1	0	0	0	1	1	1	1	0	1	0	0	0
11	0	1	0	0	0	0	1	1	0	0	1	1	1	0	0	0	0	1	1	1	0	1	0	0	0
12	0	1	0	0	1	0	1	0	1	0	0	1	1	1	0	0	0	0	1	1	1	0	0	1	0
13	0	1	0	0	1	0	1	0	1	1	1	1	1	0	0	0	0	1	1	1	1	1	1	0	0
14	0	1	0	0	0	0	1	0	1	0	1	1	1	0	0	0	0	1	1	1	1	0	0	0	0
15	0	1	0	0	0	0	1	1	0	1	1	1	1	0	0	0	0	0	1	1	0	0	1	0	0
16	0	1	0	0	1	0	1	0	1	0	1	0	1	0	0	0	0	1	1	1	0	1	0	0	0
17	0	1	0	0	1	0	1	0	0	1	1	1	1	0	0	0	0	1	0	0	0	0	1	0	0
18	1	0	0	0	0	0	0	1	0	0	1	1	1	0	0	0	0	1	1	1	0	0	1	0	0
19	0	1	0	0	0	0	0	1	0	0	1	1	1	0	0	0	1	1	1	1	0	0	1	0	0
20	0	1	0	1	0	0	1	0	0	0	1	1	1	0	0	0	1	1	1	1	0	1	0	0	0
21	0	1	0	0	1	0	1	0	0	0	1	0	1	0	0	0	1	1	1	1	0	0	0	0	0
22	0	0	1	0	0	0	0	1	0	0	1	1	0	0	0	0	0	0	1	0	0	0	0	0	0
23	0	1	0	0	1	0	1	0	0	0	1	1	1	0	0	0	0	1	1	1	0	0	0	0	0
24	0	0	1	0	0	0	1	0	0	0	1	1	1	0	0	0	0	1	1	1	0	0	0	0	0
25	0	0	1	0	1	0	1	0	1	1	1	1	0	0	0	0	0	0	1	1	0	1	0	0	0
Count	1	16	8	4	10	23	23	16	1	0	0	5	19	23	3	5	10	11	10	11	5	10	11	1	1
%	0.04	0.64	0.32	0.16	0.4	0.92	0.92	0.64	0.04	0	0	0.2	0.76	0.92	0.12	0.2	0.4	0.44	0.4	0.44	0.2	0.4	0.44	0.04	0.04

Sample Date	NOR 7A 1/12/16	#Grains 25	sa to sr to sa	Low	Medium	High	ff	pf	de	slf	cf	cg	sg	dt	crfg	as	ls	saf	up	vc	er	bb	af
1	0	1	0	0	1	0	1	0	0	1	1	0	0	0	1	0	0	0	0	0	0	1	0
2	0	1	0	0	1	0	0	0	0	1	1	0	0	0	0	1	0	0	0	0	0	1	0
3	0	1	0	0	0	1	0	0	1	0	1	0	0	0	0	0	0	1	0	1	0	0	0
4	0	1	0	0	1	0	0	1	0	0	1	0	0	0	1	1	1	0	0	1	0	0	0
5	0	0	1	0	1	0	0	0	1	0	0	0	0	0	0	0	0	0	1	0	0	0	0
6	0	1	0	0	0	1	0	1	0	1	1	0	0	0	0	1	1	0	0	1	1	0	0
7	0	0	1	0	0	0	0	1	0	1	1	0	0	1	0	0	0	0	0	0	1	0	0
8	0	1	0	0	0	1	1	1	1	0	1	0	0	0	0	1	0	0	0	1	0	0	0
9	0	1	0	0	1	0	0	1	0	1	1	0	0	0	0	0	1	0	0	0	0	0	0
10	0	1	0	0	1	0	0	1	0	1	1	0	0	0	0	1	0	0	0	0	0	0	0
11	0	1	0	0	1	0	0	1	0	0	0	0	0	0	0	0	1	0	1	0	0	0	0
12	0	1	0	0	1	0	1	0	0	0	1	0	0	0	0	1	0	0	1	0	0	0	0
13	0	1	0	0	1	0	1	0	0	1	1	1	0	0	0	1	1	0	0	0	0	1	0
14	0	1	0	0	0	1	0	1	0	1	1	0	0	0	0	1	1	0	0	0	0	0	0
15	0	0	1	0	0	1	1	0	1	1	1	0	1	0	0	0	0	1	1	1	0	0	0
16	0	0	1	0	1	0	0	0	0	1	1	0	0	0	0	1	1	0	0	1	0	0	1
17	0	0	1	0	1	0	0	0	0	0	1	0	0	0	1	1	1	0	1	0	0	0	0
18	0	0	1	0	1	0	1	0	0	1	1	0	0	0	0	1	0	0	1	0	0	1	0
19	0	1	0	0	1	0	0	1	0	0	1	0	0	0	0	1	1	0	0	0	0	0	0
20	0	0	1	0	1	0	0	0	1	0	1	0	0	0	0	0	1	1	0	0	0	0	0
21	0	0	1	0	1	0	0	0	1	0	1	0	0	0	0	1	0	0	0	0	1	1	0
22	0	0	1	0	0	1	0	0	0	0	0	0	0	1	0	0	1	1	0	0	1	0	0
23	0	0	1	0	1	0	0	0	1	1	1	0	0	0	0	0	0	1	0	0	0	0	0
24	0	0	1	0	0	1	0	0	0	0	1	0	0	0	0	0	1	0	0	1	0	0	1
25	0	0	1	0	1	0	1	1	0	0	1	0	0	0	0	0	1	0	0	1	0	0	0
Count	0	10	15	0	17	8	7	10	8	12	22	1	1	2	3	13	15	4	8	9	6	3	3
%	0	0.4	0.6	0	0.68	0.32	0.28	0.4	0.32	0.48	0.88	0.04	0.04	0.08	0.12	0.52	0.6	0.16	0.32	0.36	0.24	0.12	0.12

Sample Date	NOR 7B 10/18/15	#Grains	25	sa to	Low	Medium	High	ff	pf	de	slf	cf	cg	sg	dt	crfg	as	ls	saf	up	vc	er	bb	af
#	r to sr	sr to sa																						
1	0	0	1	0	1	0	0	0	0	0	1	1	0	0	0	0	1	0	0	0	0	1	0	0
2	0	1	0	0	1	0	0	0	0	1	1	1	0	0	0	1	1	1	0	0	0	1	1	0
3	0	1	0	0	0	0	1	0	1	1	1	1	0	0	0	0	1	1	0	0	0	0	0	0
4	0	0	1	1	0	0	0	1	0	0	1	1	0	0	0	0	0	1	0	0	0	0	0	0
5	0	1	0	1	0	0	0	0	1	0	0	1	0	0	0	1	1	1	0	0	0	0	0	0
6	0	0	1	0	0	0	0	0	1	1	1	1	0	0	0	0	0	1	0	0	0	0	0	0
7	0	1	0	0	0	0	0	1	0	1	0	1	0	0	0	0	1	1	0	0	0	1	0	0
8	0	1	0	0	0	0	1	0	1	1	0	1	1	0	0	0	1	0	0	0	0	0	0	0
9	0	0	1	0	0	0	0	0	0	0	1	1	0	0	0	0	0	1	1	0	0	0	0	0
10	0	1	0	0	0	0	1	0	1	1	0	1	0	0	0	0	1	1	0	0	0	1	0	0
11	0	0	1	0	0	0	1	0	0	1	0	1	0	0	0	0	1	1	0	0	0	0	0	0
12	0	1	0	0	0	0	1	0	1	1	0	1	0	0	0	0	0	1	0	0	0	1	0	1
13	0	1	0	0	0	0	1	0	0	1	1	1	0	0	0	0	1	1	0	0	0	0	0	0
14	0	0	1	0	0	0	1	0	1	0	0	1	0	0	0	0	0	1	1	0	0	0	0	0
15	0	1	0	0	0	0	1	0	0	1	0	1	0	0	0	1	0	1	0	0	0	0	0	0
16	0	0	1	0	0	0	1	0	0	1	0	1	0	0	0	0	1	1	0	0	0	1	0	0
17	0	0	1	0	0	0	1	0	0	1	0	1	0	0	0	0	0	1	0	0	0	1	0	0
18	0	1	0	0	0	0	1	0	0	1	0	0	0	0	0	0	0	1	0	0	0	1	0	0
19	0	0	1	0	0	0	1	0	0	1	0	1	0	0	0	0	1	0	0	0	0	0	0	0
20	0	1	0	0	0	0	1	0	0	1	1	0	0	0	0	0	1	0	0	0	1	0	0	0
21	0	0	1	0	0	0	1	0	0	0	1	1	0	0	0	0	1	1	0	0	0	0	0	0
22	0	0	1	0	0	0	1	0	0	1	1	1	0	0	0	0	1	1	0	0	0	0	0	0
23	0	0	1	0	0	0	1	0	0	1	1	0	0	0	0	0	0	0	1	1	0	0	0	0
24	0	1	0	0	0	0	1	0	0	1	0	0	0	0	0	0	1	1	1	0	0	1	0	0
25	0	0	1	0	0	0	1	0	0	0	1	1	0	0	0	1	1	1	0	0	0	0	0	0
Count	0	12	13	2	12	11	11	5	11	18	13	21	1	1	0	4	16	20	4	1	5	9	1	1
%	0	0.48	0.52	0.08	0.48	0.44	0.44	0.2	0.44	0.72	0.52	0.84	0.04	0.04	0	0.16	0.64	0.8	0.16	0.04	0.2	0.36	0.04	0.04

Sample Date	CAI 1B 17/11/16	#Grains	25																					
#	r to sr	sr to sa	sa to	Low	Medium	High	ff	pf	de	slf	cf	cg	sg	dt	crg	as	ls	saf	up	vc	er	bb	af	
1	0	1	0	0	1	0	0	1	1	1	0	0	0	0	0	1	0	0	1	1	1	0	1	
2	0	1	0	0	1	0	0	1	1	0	0	0	0	0	1	1	0	0	1	1	1	1	0	0
3	0	0	1	0	0	1	0	0	1	1	1	1	0	0	0	1	1	0	1	1	0	0	0	
4	0	0	1	0	1	0	0	0	1	0	0	0	0	0	0	1	1	0	1	0	0	0	0	
5	0	1	0	0	1	0	0	0	1	0	0	0	0	0	0	1	1	0	1	0	0	0	0	
6	0	0	1	0	1	0	0	0	1	1	1	0	0	0	0	1	0	0	1	0	0	0	0	
7	0	1	0	0	1	0	0	0	1	0	0	0	0	0	1	1	0	1	1	0	1	0	0	
8	0	1	0	0	0	1	0	0	1	1	1	0	0	0	0	0	1	0	1	0	1	1	1	
9	0	0	1	0	0	1	0	1	1	1	0	0	0	0	0	0	0	0	0	0	0	0	0	
10	0	0	1	0	0	1	0	0	1	0	1	0	0	0	0	1	0	1	1	0	0	0	0	
11	0	1	0	0	1	0	0	0	1	1	0	0	0	0	0	1	0	0	1	1	0	0	0	
12	0	0	1	0	1	0	0	0	1	1	1	0	0	0	0	1	1	0	1	0	1	1	0	
13	0	0	1	0	0	1	0	0	1	1	1	0	0	0	0	1	1	0	1	0	0	0	0	
14	0	0	1	0	1	0	0	0	1	0	0	0	0	0	0	1	1	0	1	0	0	0	0	
15	0	0	1	0	1	0	0	0	1	1	1	0	0	0	0	0	1	1	1	0	0	0	0	
16	0	0	1	0	1	0	0	0	1	1	0	0	0	0	1	0	1	0	1	1	0	0	0	
17	0	0	1	0	1	0	0	0	1	1	1	0	0	0	0	1	0	0	0	0	0	0	0	
18	0	0	1	0	0	1	0	0	1	0	1	0	0	0	0	1	1	0	1	1	0	1	0	
19	0	1	0	0	1	0	0	0	1	0	0	0	0	0	0	0	1	0	1	1	1	0	0	
20	0	0	1	0	1	0	0	0	1	1	1	0	0	0	0	1	1	1	0	0	0	0	0	
21	0	0	1	0	0	1	0	0	1	0	0	0	0	0	0	0	1	0	1	0	0	0	0	
22	0	0	1	0	1	0	0	0	0	0	0	0	0	0	0	1	1	0	0	1	0	0	0	
23	0	0	1	0	1	0	0	0	1	0	0	0	0	0	0	1	1	0	1	0	0	1	0	
24	0	1	0	0	1	0	0	0	1	1	0	0	0	0	0	0	1	0	1	0	0	1	0	
25	0	0	1	0	1	0	0	0	1	1	0	0	0	0	0	1	1	0	1	0	0	0	0	
Count	0	8	17	0	18	7	0	10	23	13	11	0	0	0	3	18	17	4	20	8	7	5	2	
%	0	0.32	0.68	0	0.72	0.28	0	0.4	0.92	0.52	0.44	0	0	0	0.12	0.72	0.68	0.16	0.8	0.32	0.28	0.2	0.08	

Sample Date	CAI 2A 17/14/16	#Grains	25	sa to	sr to sa	High	Low	Medium	ff	pf	de	slf	cf	cg	sg	dt	crfg	as	ls	saf	up	vc	er	bb	af
1	0	0	1	0	0	1	0	0	0	0	1	1	1	0	1	0	0	0	0	0	0	0	0	0	0
2	0	1	0	0	1	0	0	1	0	0	0	1	1	0	0	0	0	0	0	0	0	0	0	1	0
3	0	0	1	0	0	1	0	0	0	0	1	0	1	0	1	0	0	0	0	0	1	0	0	0	1
4	0	0	1	0	0	0	0	0	0	1	1	1	1	0	0	0	1	0	1	0	0	0	0	0	0
5	0	1	0	0	0	1	0	0	0	0	1	0	1	0	0	0	0	0	0	0	0	0	1	0	1
6	0	0	1	0	0	1	0	0	0	0	0	0	1	0	0	0	0	0	0	0	0	0	0	0	0
7	0	0	1	0	0	1	0	0	1	0	1	1	1	0	1	0	0	0	0	0	0	0	0	0	0
8	0	0	1	0	0	0	0	1	0	0	0	0	1	0	1	0	0	1	0	0	0	0	0	0	0
9	0	1	0	0	1	0	0	1	0	0	1	0	1	0	0	0	1	1	1	0	0	0	1	0	0
10	0	1	0	0	1	0	0	0	0	0	1	1	1	0	0	1	0	0	0	0	0	0	1	0	0
11	0	1	0	0	0	0	0	1	0	0	1	0	1	0	0	0	0	1	1	0	1	0	0	0	0
12	0	1	0	0	0	1	0	0	0	0	1	1	1	0	0	0	1	1	1	0	0	0	0	0	0
13	0	1	0	0	0	0	0	1	0	0	1	1	1	0	0	0	0	0	1	0	0	0	0	0	1
14	0	0	1	0	0	0	0	1	0	0	1	1	1	0	0	0	0	0	0	0	0	0	1	0	1
15	0	1	0	0	0	0	0	1	0	0	1	0	1	0	0	0	0	0	1	0	0	1	1	0	0
16	0	1	0	0	0	1	0	0	0	0	1	0	1	0	0	0	0	0	1	0	0	1	1	0	0
17	0	0	1	0	0	0	0	1	0	0	1	1	0	0	0	0	1	0	1	0	1	0	0	0	0
18	0	0	1	0	0	1	0	0	0	0	1	0	1	0	0	0	1	0	0	0	0	0	0	0	0
19	0	1	0	0	0	0	0	1	0	0	0	1	1	0	0	0	0	0	0	1	0	0	0	0	0
20	1	0	0	0	0	0	0	0	0	0	1	1	1	0	0	0	0	1	1	0	0	0	1	0	1
21	0	1	0	0	0	0	0	0	0	1	1	1	0	0	0	0	0	1	1	0	0	0	0	0	0
22	0	1	0	0	0	0	0	1	0	0	1	1	1	0	1	0	1	0	1	0	0	0	1	0	0
23	0	1	0	0	0	0	0	0	0	0	1	1	1	0	0	0	0	0	1	0	0	0	0	0	0
24	0	0	1	0	0	0	0	1	0	0	1	0	0	0	0	0	0	1	1	0	0	0	0	1	1
25	0	0	0	1	0	0	0	0	0	1	1	1	1	0	0	0	0	1	1	0	1	0	0	0	0
Count	1	12	12	0	11	13	6	21	15	22	0	5	1	6	8	16	24	32	64	0.04	0.16	0.08	0.36	0.04	0.28
%	0.04	0.48	0.48	0	0.44	0.52	0.04	0.84	0.6	0.88	0	0.2	0.04	0.24	0.32	0.64	0.24	0.32	0.64	0.04	0.16	0.08	0.36	0.04	0.28

Sample Date	CAL 28 10/17/15	#Grains	25	sa to	Low	Medium	High	ff	pf	de	slf	cf	cg	sg	dt	crfg	as	ls	saf	up	vc	er	bb	af
#	r to sr	sr to sa	sa to	Low	Medium	High	ff	pf	de	slf	cf	cg	sg	dt	crfg	as	ls	saf	up	vc	er	bb	af	
1	0	1	0	0	1	0	0	0	1	1	1	1	0	0	0	0	1	0	0	0	0	1	0	0
2	0	1	0	0	1	0	0	0	0	1	0	1	0	0	1	0	1	1	1	0	0	0	1	0
3	0	0	1	0	0	1	0	0	1	1	1	1	0	0	0	0	1	1	0	0	0	0	0	0
4	0	0	1	1	0	0	1	1	1	1	1	0	0	0	0	0	0	0	1	1	0	0	0	0
5	0	0	1	0	1	0	0	0	0	1	0	1	0	0	0	0	0	1	1	0	0	0	0	0
6	0	1	0	0	0	0	0	0	1	1	0	1	0	0	0	0	1	1	1	1	1	0	0	1
7	0	1	0	0	0	0	0	0	0	1	1	1	0	0	0	0	1	1	1	1	0	1	0	0
8	0	1	0	0	0	1	0	0	0	1	1	1	0	0	1	0	1	1	1	0	0	0	0	0
9	0	1	0	0	1	0	0	0	0	1	1	1	0	0	1	0	0	0	0	0	1	1	0	0
10	0	0	1	0	1	0	0	0	0	1	1	1	0	0	0	1	1	0	1	0	0	0	0	0
11	0	0	1	0	1	0	0	0	0	1	1	1	0	0	0	0	1	0	0	0	0	0	0	1
12	0	1	0	0	0	1	0	0	1	0	1	0	1	0	0	0	0	1	0	0	0	0	0	1
13	0	0	1	0	0	0	1	0	0	1	1	0	0	0	1	1	1	1	1	0	1	0	0	0
14	0	1	0	0	0	0	0	0	0	1	0	1	0	0	1	0	1	1	0	1	0	0	0	0
15	0	0	1	0	0	0	0	0	1	1	1	1	0	0	0	0	0	1	0	1	0	0	0	0
16	0	0	1	0	0	1	0	0	0	1	1	1	0	0	0	0	1	0	0	1	0	0	0	0
17	0	1	0	0	0	1	0	0	1	1	1	1	0	0	1	1	1	1	0	0	0	0	0	0
18	0	0	1	0	1	0	0	0	0	1	1	0	1	0	0	0	0	0	0	0	0	1	0	0
19	0	0	1	0	1	0	0	0	0	1	1	0	0	0	0	1	1	1	1	0	1	0	0	1
20	0	0	1	0	1	0	0	0	0	0	1	1	0	0	0	1	1	1	1	1	0	0	0	1
21	0	0	1	0	0	1	0	0	1	1	1	1	0	0	0	1	1	0	0	0	0	0	0	0
22	0	0	1	0	0	0	1	0	0	1	1	1	0	0	0	1	1	0	0	1	1	0	0	0
23	0	0	1	0	1	0	0	0	0	1	0	1	0	0	0	1	1	1	0	0	0	0	1	0
24	0	0	1	0	0	0	1	0	1	1	1	0	0	0	1	0	0	1	0	0	1	0	0	0
25	0	0	1	0	0	0	1	0	0	1	1	1	0	0	0	0	0	1	0	0	0	1	0	0
Count	0	8	17	1	11	13	1	6	23	19	20	2	2	2	7	15	16	8	9	6	5	3	5	
%	0	0.32	0.68	0.04	0.44	0.52	0.04	0.24	0.92	0.76	0.8	0.08	0.08	0.08	0.28	0.6	0.64	0.32	0.36	0.24	0.2	0.12	0.2	

Sample Date	CAI 3A 1/6/16	# Grains	25																					
#	r to sr	sr to sa	sa to	Low	Medium	High	ff	pf	de	sif	cf	cg	sg	dt	crg	as	ls	saf	up	vc	er	bb	af	
1	0	0	1	0	1	0	0	1	1	1	0	0	0	0	0	0	0	0	1	1	0	0	0	
2	0	0	1	1	0	0	0	0	0	1	0	0	0	0	0	0	1	0	1	0	0	0	0	
3	0	0	1	0	0	1	0	1	1	0	1	0	0	0	0	0	0	0	0	0	1	0	0	
4	0	0	1	0	1	0	0	0	1	1	1	0	0	0	1	0	0	1	0	1	0	1	0	
5	0	0	1	0	1	0	0	1	1	1	1	0	0	0	1	0	0	0	0	0	0	1	0	
6	0	0	1	0	1	0	0	1	1	1	1	0	1	0	0	1	0	1	0	0	1	0	1	
7	0	0	1	1	0	0	0	0	1	0	1	0	0	0	1	1	0	1	0	1	1	0	0	
8	0	0	1	0	1	0	0	0	1	1	1	0	0	0	0	0	1	0	0	0	0	0	0	
9	0	0	1	0	0	0	0	0	1	0	1	0	0	0	1	0	0	0	1	0	1	0	0	
10	0	0	1	0	1	0	0	0	0	1	1	0	0	0	0	0	1	0	1	0	0	0	0	
11	0	0	1	0	0	0	0	0	1	1	1	0	0	0	0	0	0	0	1	0	0	0	0	
12	0	0	1	0	0	0	0	1	1	1	1	0	0	0	0	0	0	0	0	0	1	1	0	
13	0	0	1	0	1	0	0	1	1	0	0	0	0	0	0	0	0	1	0	0	0	0	0	
14	0	0	1	0	1	0	0	0	1	1	1	0	0	0	1	0	0	0	1	0	0	0	0	
15	0	0	1	0	0	1	0	0	1	0	1	0	0	0	0	0	0	0	0	0	1	0	1	
16	0	0	1	0	1	0	0	0	1	0	1	0	0	0	0	0	1	0	0	1	0	0	0	
17	0	0	1	0	1	0	0	1	1	1	1	0	0	0	0	1	0	0	0	1	0	0	1	
18	0	0	1	0	1	0	0	0	0	1	1	0	0	0	0	1	0	1	0	0	0	0	0	
19	0	0	1	0	1	0	0	1	1	1	0	0	0	0	0	1	1	0	1	0	0	0	0	
20	0	0	1	0	0	1	0	0	1	0	0	0	0	0	0	0	1	0	0	0	0	1	1	
21	0	0	1	0	0	0	0	0	1	1	0	0	0	0	0	0	1	0	0	0	0	1	0	
22	0	0	1	1	0	0	0	0	0	1	0	0	0	0	1	0	1	0	0	1	0	0	1	
23	0	0	1	0	1	0	0	0	1	1	1	0	0	0	0	1	0	0	1	1	0	0	0	
24	0	0	1	0	1	0	0	0	1	1	1	0	0	0	0	0	0	1	1	1	0	0	0	
25	0	0	1	0	0	1	0	0	1	0	1	0	0	0	0	1	0	0	0	0	0	1	0	0
Count	0	6	19	4	18	2	1	9	21	17	17	0	0	0	5	7	9	5	9	11	7	5	5	
%	0	0.24	0.76	0.16	0.72	0.08	0.04	0.36	0.84	0.68	0.68	0	0.04	0	0.2	0.28	0.36	0.2	0.36	0.44	0.28	0.2	0.2	

Sample Date	CAI 4B 12/15/15	# Grains	25	
#	r to sr	sr to sa	sa to	
	Low	Medium	High	
1	0	0	1	1
2	0	0	1	0
3	0	0	1	1
4	0	0	1	1
5	0	0	1	1
6	0	0	1	1
7	0	0	1	1
8	0	0	1	1
9	0	0	1	0
10	0	0	1	0
11	0	0	1	1
12	0	0	1	1
13	0	0	1	1
14	0	0	1	1
15	0	0	1	1
16	0	0	1	1
17	0	0	1	1
18	0	0	1	1
19	0	0	1	1
20	0	0	1	0
21	0	0	1	0
22	0	0	1	0
23	0	0	1	0
24	0	0	1	0
25	0	0	1	0
Count	0	10	15	7
%	0	0.4	0.6	0.28
	ff	pf	de	sif
	cf	cg	sg	dt
	crg	as	ls	saf
	up	vc	er	bb
	af			

Sample Date	CAI SA 9/15/15	# Grains	25																				
#	r to sr	sr to sa	sa to	Low	Medium	High	ff	pf	de	sif	cf	cg	sg	dt	crg	as	ls	saf	up	vc	er	bb	af
1	0	0	1	0	1	0	0	0	0	1	1	0	0	0	0	1	0	0	1	1	1	0	0
2	0	0	1	0	1	0	0	0	1	1	1	0	0	0	0	0	1	1	1	0	1	0	0
3	0	0	1	1	0	0	0	0	0	1	0	0	0	0	1	0	0	0	0	0	0	1	0
4	0	0	1	0	0	1	0	1	1	1	1	0	0	0	0	0	0	0	0	0	0	0	0
5	0	0	1	0	1	0	0	0	1	1	1	0	0	0	0	1	1	1	1	1	0	0	0
6	0	0	1	0	0	1	0	0	0	1	1	0	0	0	0	0	1	1	1	1	0	0	0
7	0	0	1	0	0	1	0	0	1	1	1	0	0	0	0	0	1	1	0	1	0	0	0
8	0	0	1	0	1	0	1	0	1	1	1	0	0	0	0	1	1	1	0	0	1	0	0
9	0	0	1	0	1	0	0	0	1	1	1	0	0	0	0	0	1	1	1	1	1	0	0
10	0	0	1	0	1	0	0	0	0	1	1	0	0	0	0	1	0	0	0	0	0	0	0
11	0	1	0	0	1	0	0	0	1	1	1	0	0	0	0	1	0	0	1	1	1	0	0
12	0	0	1	0	0	1	0	0	1	1	1	0	0	0	1	1	1	0	0	0	1	0	0
13	0	0	1	0	0	1	0	0	0	1	1	0	0	0	0	1	1	0	1	1	0	0	0
14	0	0	1	0	0	1	0	1	1	1	1	0	0	0	0	1	1	0	0	1	1	0	0
15	0	1	0	0	1	0	0	0	0	1	0	0	0	0	0	1	1	0	1	0	1	0	0
16	0	0	1	0	1	0	0	0	1	0	1	0	0	0	0	1	1	0	1	0	0	0	0
17	0	1	0	0	1	0	0	0	0	1	1	0	0	0	1	1	1	0	1	0	1	0	0
18	0	0	1	0	0	1	0	0	1	1	1	0	0	0	0	1	1	0	0	0	0	0	0
19	0	0	1	0	0	0	0	0	1	0	1	0	0	0	1	1	0	0	0	1	0	0	1
20	0	0	1	0	1	0	0	1	1	1	1	0	0	0	0	0	0	0	0	1	1	0	0
21	0	0	1	0	0	1	0	0	1	1	1	0	0	0	0	1	1	1	0	0	0	0	1
22	0	0	1	0	1	0	0	0	0	1	0	0	0	0	0	0	0	0	1	1	0	0	0
23	0	0	1	0	1	0	1	0	0	1	1	0	0	0	0	0	0	1	1	1	0	0	0
24	0	0	1	0	0	1	0	0	1	1	1	0	0	0	0	1	1	0	0	0	0	1	0
25	0	0	1	0	1	0	0	0	1	0	1	0	0	0	0	1	0	0	0	1	1	0	0
Count	0	3	22	1	14	10	2	3	16	22	19	0	0	0	4	17	14	4	10	11	8	4	2
%	0	0.12	0.88	0.04	0.56	0.4	0.08	0.12	0.64	0.88	0.76	0	0	0	0.16	0.68	0.56	0.16	0.4	0.44	0.32	0.16	0.08

Sample Date	CAI 5B 12/16/15	# Grains	25																						
#	r to sr	sr to sa	sa to	Low	Medium	High	ff	pf	de	sif	cf	cg	sg	dt	crg	as	ls	saf	up	vc	er	bb	af		
1	0	0	1	0	0	1	0	1	1	0	1	0	0	0	0	1	0	0	0	0	0	0	1		
2	0	0	1	0	1	0	0	1	1	1	1	0	0	0	0	0	1	1	0	1	0	1	0	0	
3	0	0	1	0	0	1	0	0	1	1	1	0	0	0	0	0	0	1	0	0	0	0	0	0	
4	0	1	0	0	1	0	0	1	1	0	1	0	0	0	0	0	1	0	1	1	1	0	0	0	
5	0	1	0	0	0	1	0	0	1	0	0	0	0	0	0	0	0	0	0	0	0	0	1	0	0
6	0	1	0	0	1	0	0	0	1	1	1	0	0	0	0	1	0	0	1	0	0	0	0	0	0
7	0	1	0	0	0	1	0	0	1	1	1	0	0	0	1	1	0	0	0	0	0	0	0	0	0
8	0	0	1	0	0	1	0	0	1	1	0	0	0	0	0	1	1	0	0	1	0	0	0	1	
9	0	1	0	0	0	1	0	0	1	1	1	0	0	0	0	0	1	0	0	0	1	0	0	0	
10	0	0	1	0	1	0	0	0	1	1	1	0	0	0	1	0	0	0	1	1	0	0	0	0	
11	0	1	0	0	1	0	0	0	0	0	1	0	0	0	1	1	0	0	0	0	0	0	0	0	
12	0	0	1	0	1	0	0	0	0	0	1	0	0	0	0	0	0	0	0	0	0	0	0	0	
13	0	0	1	0	1	0	0	0	1	0	1	0	0	0	0	0	1	0	0	0	0	0	1	0	
14	0	1	0	0	1	0	0	0	1	0	1	0	0	0	0	1	1	1	1	0	0	0	0	0	
15	0	1	0	0	1	0	0	0	1	1	1	0	0	0	0	0	0	0	1	0	0	0	0	0	
16	0	1	0	0	1	0	0	0	1	1	1	0	0	0	0	0	1	0	0	0	0	0	0	0	
17	0	0	1	0	0	1	0	1	1	1	1	0	0	0	1	0	0	0	0	0	0	0	0	0	
18	0	0	1	0	1	0	0	0	0	1	1	0	0	0	0	1	0	0	0	1	1	0	0	0	
19	0	0	1	0	0	1	0	0	1	0	0	0	0	0	0	1	0	0	1	0	0	0	0	0	
20	0	1	0	0	1	0	0	0	1	1	0	0	0	0	1	0	1	0	1	1	1	0	0	0	
21	0	1	0	0	0	1	0	0	1	1	1	0	0	1	0	1	0	0	1	0	1	0	0	1	
22	0	1	0	0	1	0	0	1	1	0	1	0	0	0	0	0	0	0	0	1	0	0	0	0	
23	0	1	0	0	1	0	0	0	1	0	1	0	0	0	0	0	0	0	1	0	0	0	0	0	
24	0	0	1	0	1	0	0	0	1	1	1	0	0	0	1	0	0	0	1	0	1	0	0	0	
25	0	0	1	0	1	0	0	0	1	1	1	0	0	0	0	1	0	0	0	1	0	0	0	1	
Count	0	12	13	0	16	9	0	6	22	16	20	0	0	1	6	12	9	1	11	7	5	2	4		
%	0	0.48	0.52	0	0.64	0.36	0	0.24	0.88	0.64	0.8	0	0	0.04	0.24	0.48	0.36	0.04	0.44	0.28	0.2	0.08	0.16		

Sample Date	PR 2B 3/13/16	# Grains	25	
#	r to sr	sr to sa	sa to	
	Low	Medium	High	
1	0	0	1	1
2	0	0	1	1
3	0	0	1	0
4	0	0	1	1
5	0	0	1	1
6	0	0	1	1
7	0	0	1	1
8	0	0	1	1
9	0	0	1	1
10	0	0	1	0
11	0	0	1	1
12	0	0	1	1
13	0	0	1	1
14	0	0	1	1
15	0	0	1	1
16	0	0	1	1
17	0	0	1	1
18	0	0	1	1
19	0	0	1	0
20	0	0	1	1
21	0	0	1	1
22	0	0	1	1
23	0	0	1	1
24	0	0	1	1
25	0	0	1	1
Count	0	10	15	13
%	0	0.4	0.6	0.52
	ff	pf	de	sif
	cf	cg	sg	dt
	crg	as	ls	saf
	up	vc	er	bb
	af			

Sample Date	PR 4B 9/16/15	#Grains	25
#	r to sr	sr to sa	sa to
1	0	0	1
2	0	1	0
3	0	0	1
4	0	0	1
5	0	1	0
6	0	0	1
7	0	0	1
8	0	0	1
9	0	0	1
10	0	1	0
11	0	1	0
12	0	1	0
13	0	1	0
14	0	0	1
15	0	0	1
16	0	1	0
17	0	1	0
18	0	1	0
19	0	0	1
20	0	0	1
21	0	1	0
22	0	0	1
23	0	0	1
24	0	1	0
25	0	0	1
Count	0	10	15
%	0	0.4	0.6
	ff	pf	de
	slf	cf	cg
	sg	dt	crf
	as	ls	saf
	up	vc	er
	bb	af	
	12	11	10
	0.92	0.72	0.88
	0.16	0.22	0.22
	0	0	0
	0.04	0.04	0
	0	0	0
	0.52	0.13	0.18
	0.48	0.12	0.16
	0	0	0
	0.48	0.52	0.64
	0	0	0
	0.6	0.4	0.1
	0.4	0.6	0.1
	0.04	0.04	0
	0.2	0.2	0.2
	0.6	0.15	0.15
	0.4	0.4	0.4
	0.04	0.04	0.04
	0.2	0.2	0.2
	0.04	0.04	0.04
	0.1	0.1	0.1

Sample Date	PR 6A 1/18/16	#Grains	24																					
#	r to sr	sr to sa	sa to	Low	Medium	High	ff	pf	de	sif	cf	cg	sg	dt	crq	as	ls	saf	up	vc	er	bb	af	
1	0	0	1	0	1	0	0	0	0	1	0	0	0	0	0	0	1	0	0	0	0	0	1	
2	0	0	1	0	0	1	1	0	1	1	1	0	0	0	0	1	0	0	0	0	0	0	0	0
3	0	0	1	0	1	0	0	1	1	0	1	1	0	0	0	0	1	0	0	0	0	1	0	0
4	0	1	0	0	1	0	0	0	1	1	0	0	0	0	0	1	1	0	0	0	1	0	0	1
5	0	0	1	0	1	0	0	0	1	1	0	0	0	0	0	1	1	1	0	0	0	0	0	0
6	0	0	1	0	1	0	0	0	1	1	1	0	0	0	0	1	1	1	0	0	0	0	0	0
7	0	0	1	0	1	0	0	0	1	1	1	0	0	0	1	1	1	1	0	0	1	0	0	0
8	0	1	0	0	1	0	0	0	1	1	0	0	0	0	0	1	1	0	1	0	1	0	0	0
9	0	0	1	0	0	1	0	0	1	1	0	0	0	0	1	0	1	1	0	0	0	0	0	0
10	0	0	1	0	0	1	0	0	1	1	0	0	0	0	0	1	0	0	0	0	0	0	0	0
11	0	1	0	0	1	0	0	0	1	1	0	0	0	0	0	0	1	0	1	1	1	0	0	0
12	0	1	0	0	0	1	0	0	1	1	1	0	0	0	0	0	1	0	0	0	0	0	0	0
13	0	1	0	0	0	1	0	0	1	1	1	0	0	0	0	1	1	0	0	0	1	0	0	0
14	0	1	0	0	0	1	0	0	1	0	1	0	0	0	0	1	1	0	0	0	0	0	0	0
15	0	0	1	0	1	0	0	0	1	0	0	0	0	0	0	1	1	0	0	0	0	0	0	0
16	0	1	0	0	0	1	0	0	1	1	0	0	0	0	0	1	0	0	0	0	0	0	0	0
17	0	0	1	0	0	1	0	0	1	1	1	0	0	0	1	1	1	0	0	0	1	0	0	0
18	0	0	1	0	0	1	0	0	1	1	1	0	0	0	0	0	0	0	0	0	1	0	0	0
19	0	1	0	0	1	0	0	0	1	1	1	0	0	0	1	1	1	0	0	1	1	0	0	0
20	0	1	0	0	1	0	0	0	1	0	0	0	0	0	1	0	1	0	1	0	0	0	0	0
21	0	1	0	0	0	1	0	0	1	1	0	0	0	1	0	1	1	0	1	1	1	0	0	1
22	0	0	1	0	0	1	0	0	1	0	0	0	0	0	0	0	1	0	0	1	0	0	0	0
23	0	0	1	0	1	0	0	0	1	1	0	0	0	0	1	0	0	0	0	1	1	0	0	0
24	0	0	1	0	0	1	0	0	1	0	0	0	1	0	0	1	1	0	0	0	0	0	0	1
25	0	0	1	0	0	1	0	0	1	0	0	0	0	0	0	0	0	0	0	0	0	0	0	0
Count	0	10	14	0	13	11	1	9	23	18	9	1	1	1	5	16	19	5	4	9	9	0	4	0
%	0	0.41667	0.58333	0	0.54167	0.45833	0.0417	0.375	0.95833	0.75	0.375	0.04167	0.04167	0.04167	0.20833	0.66667	0.79167	0.20833	0.16667	0.375	0.375	0	0.16667	0

Sample Date	PERU1B 3/29/16	# Grains	25	
#	r to sr	sr to sa	sa to	
	Low	Medium	High	
1	0	0	1	0
2	0	0	1	0
3	0	1	0	1
4	0	1	0	1
5	0	1	0	1
6	0	1	0	1
7	0	1	0	1
8	0	1	0	1
9	0	1	0	1
10	1	0	0	1
11	0	1	0	1
12	0	1	0	1
13	0	1	0	1
14	0	1	0	1
15	0	1	0	1
16	0	1	0	1
17	0	1	0	1
18	0	1	0	1
19	0	1	0	1
20	0	1	0	1
21	0	1	0	1
22	0	1	0	1
23	0	1	0	1
24	0	1	0	1
25	0	1	0	1
Count	1	13	11	4
%	0.04	0.52	0.44	0.16
	17	18	17	1
	0.68	0.72	0.68	0.04
	de	sif	cf	cg
	0	1	1	0
	17	18	17	0
	0.68	0.72	0.68	0
	3	6	7	11
	0.12	0.24	0.28	0.44
	dt	crg	as	ls
	0	1	1	0
	0	0.24	0.28	0.44
	sg			
	0	0.04	0	0.04
	1	3	6	7
	0.04	0.12	0.24	0.28
	up	saf	vc	er
	0	0	1	0
	0.32	0.12	0.16	0.24
	8	3	4	6
	0.32	0.12	0.16	0.24
	bb	af		
	0	0	1	0
	0.08	0.08	2	0.08

Sample Date	PERU 2B 3/29/16	# Grains	25																				
#	r to sr	sr to sa	sa to	Low	Medium	High	ff	pf	de	sif	cf	cg	sg	dt	crg	as	ls	saf	up	vc	er	bb	af
1	0	1	0	0	1	0	1	0	1	1	1	0	0	0	0	0	1	0	0	1	0	0	0
2	0	0	1	0	1	0	1	0	0	1	0	0	0	0	0	1	1	0	0	0	1	0	0
3	0	1	0	0	1	0	0	0	1	0	1	0	0	0	0	0	1	0	1	0	0	0	0
4	0	0	1	0	0	1	0	0	1	0	0	0	0	0	0	1	0	1	0	0	0	0	0
5	0	0	1	0	0	1	0	1	1	1	0	0	0	0	0	0	1	0	0	1	0	1	0
6	0	1	0	0	1	0	0	1	1	1	1	0	0	0	0	0	0	1	0	1	1	0	0
7	0	0	1	0	0	1	0	0	1	1	1	0	0	0	1	0	0	1	1	1	1	0	0
8	0	1	0	0	1	0	0	1	1	0	1	0	0	0	0	0	1	0	1	0	1	0	0
9	0	0	1	0	0	1	0	0	0	1	1	0	0	0	0	0	1	0	1	0	0	0	0
10	0	0	1	0	0	1	0	0	1	1	1	0	0	0	1	0	0	0	0	0	0	0	0
11	0	1	0	0	0	1	0	1	1	0	1	0	0	0	0	1	1	0	1	0	1	0	0
12	0	0	1	0	0	1	1	1	0	1	1	0	0	0	0	0	1	1	1	0	0	0	0
13	0	0	1	0	0	1	0	1	1	1	1	0	0	0	0	1	0	0	0	0	0	0	0
14	1	0	0	0	0	1	0	1	1	1	0	0	0	0	0	0	1	0	1	0	1	0	0
15	0	1	0	0	0	1	1	0	1	1	1	0	0	0	0	1	0	0	0	0	0	0	0
16	0	0	1	0	1	0	0	0	1	1	1	0	0	0	0	0	1	0	1	0	0	0	0
17	0	1	0	0	0	1	0	0	1	1	1	0	0	0	0	0	1	0	1	0	1	0	0
18	0	0	1	0	1	0	0	0	0	1	1	0	0	0	0	0	0	0	0	0	0	0	0
19	0	1	0	0	1	0	0	0	1	0	1	0	0	0	0	0	1	0	1	0	1	0	0
20	0	1	0	0	1	0	0	0	1	1	1	0	0	0	1	0	1	0	1	0	0	0	0
21	0	0	1	0	0	1	1	0	1	1	1	0	0	0	0	0	0	0	0	0	0	0	0
22	0	1	0	0	0	1	0	0	1	1	1	0	0	0	0	1	1	0	0	0	0	0	0
23	0	0	1	0	1	0	1	0	0	1	1	0	1	0	0	0	1	0	0	0	0	0	0
24	0	1	0	0	1	0	0	1	1	1	1	0	0	0	0	1	1	0	0	1	1	0	0
25	0	1	0	0	1	0	0	0	1	1	1	0	0	0	0	1	1	0	1	0	1	0	0
Count	1	12	12	0	12	8	7	8	19	20	21	0	1	0	3	8	18	3	12	5	9	1	0
%	0.04	0.48	0.48	0	0.48	0.32	0.28	0.32	0.76	0.8	0.84	0	0.04	0	0.12	0.32	0.72	0.12	0.48	0.2	0.36	0.04	0